DIPARTIMENTO di ELETTRONICA, INFORMAZIONE e BIOINGEGNERIA

POLITECNICO DI MILANO





Lecture 5
Resistive sensors: mechanical (stress/strain), light (LDR), magnetoresistors

Resistive sensors

- **Mechanical**
  force/pressure (strain gauges, piezoresistances)
- **Optical**
  light detectors (LDR)
- **Magnetic**
  magnetoresistors
- **Thermal**
  temperature sensors (RTD, NTC thermistors, PTC thermistors)
- **Chemical**
  resistive gas sensors, resistive hygrometers

Materials for resistive sensors

- **Mechanical**
  strain gauges: metallic alloys ($Cu_{55}Ni_{45}$, $Cu_{57}Ni_{43}$,…)
  piezoresistances: semiconductors (Si, Ge)

- **Optical**
  LDR: semiconductors (CdS. PbS, PbSe)

- **Magnetic**
  magnetoresistors: metallic alloys ($Ni_{80}Fe20$, Ni-Fe-Co),
  semicond. (InSb, InAs)

- **Thermal**
  RTD: metals (Pt, Cu, Ni, Mb)
  NTC thermistors: Ni, Co, Fe oxides
  PTC thermistors: ceramics (e.g.: barium titanate)

- **Chemical**
  resistive gas sensors: semiconductors, metal oxides, conductive polymers
  resistive hygrometers: salts (LiCl, BaF_2), conductive polymers

Resistive sensors of force, pressure, stress, strain

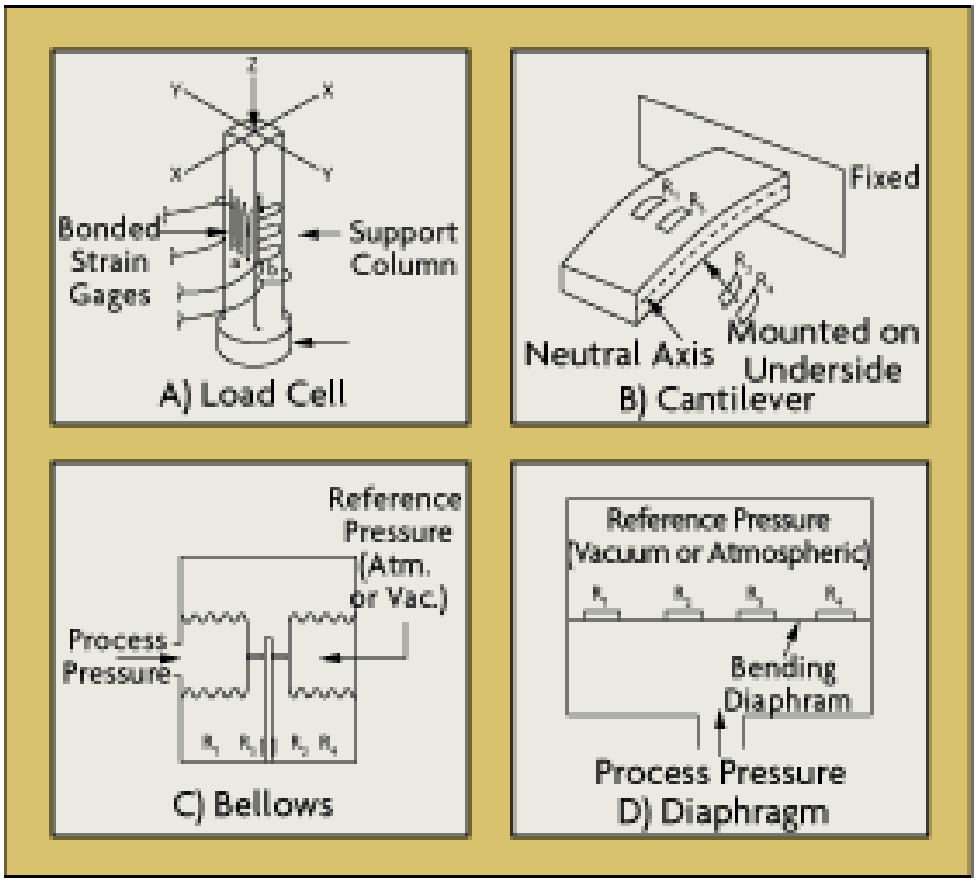

Examples of application:

⇒ devices for blood pressure measurement

⇒ mechanical ventilators

⇒ sensorized surgical instruments

⇒ sensorized prostheses

⇒ atomic force microscopy (AFM)

Piezo-resistance fundamentals

The electrical resistance R of a homogeneous structure is a function of its dimensions and resistivity

$$\mathrm{R} = \rho \frac{\ell}{\mathrm{A}}$$

A longitudinal mechanical stress produces a change in resistance that depends on resistivity ρ, length ℓ and cross sectional area A:

$$dR = \frac{\rho d\ell}{A} + \frac{\ell d\rho}{A} - \frac{\rho \ell dA}{A^2} = \frac{A\left(\rho d\ell + \ell d\rho\right) - \rho \ell dA}{A^2}$$

$$\frac{dR}{R} = \frac{A\left(\rho d\ell + \ell d\rho\right) - \rho \ell dA}{A^2} \cdot \frac{A}{\rho \ell} = \frac{d\ell}{\ell} + \frac{d\rho}{\rho} - \frac{dA}{A}$$

The change of length ℓ of a material in which cross sectional area is A and on which a force F is applied, is given by Hooke's law:

$$\sigma = \frac{F}{A} = E\varepsilon = E\frac{d\ell}{\ell}$$

where E è Young's modulus, σ is the applied stress and ε is the strain (adimensional, m/m or $\mu\varepsilon=10^{-6}$ m/m)

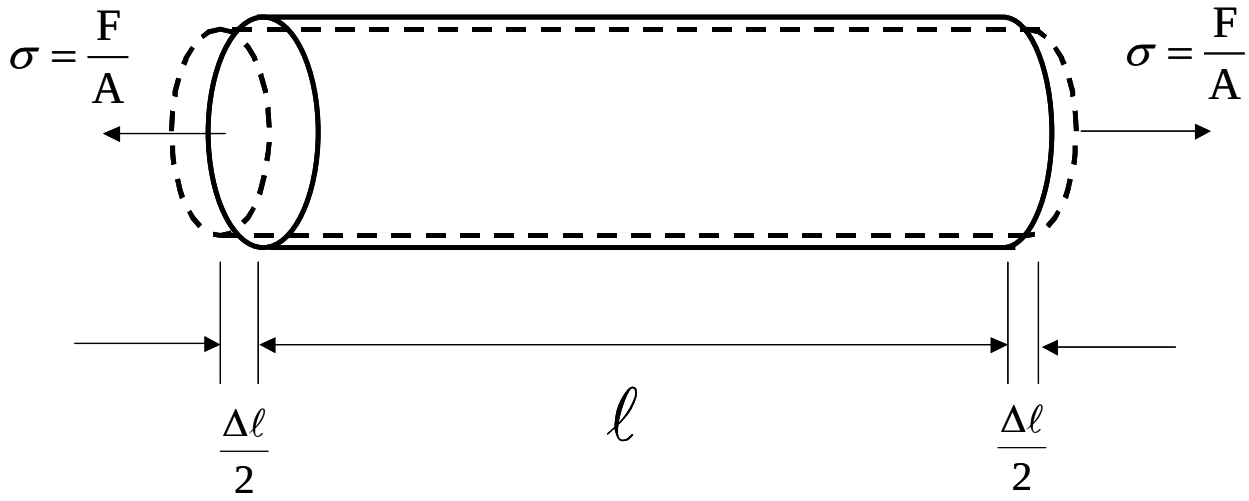

The change in resistance due to applied stress is a function of geometry and resistivity changes. The cross-sectional area of a bulk material reduces in proportion to the longitudinal strain by its Poisson's ratio, which for most metals ranges from 0.20 to 0.35.

For anisotropic silicon, the effective directional Poisson's ratio ranges from 0.06 to 0.36 . The isotropic lower and upper limit for are 1.0 and 0.5.

The cross-sectional area of a bulk material reduces in proportion to the longitudinal strain by its **Poisson's ratio ν**, which for most metals ranges from 0.20 to 0.35.

$$\nu = -\frac{dt/t}{d\ell/\ell}$$

(t=transversal dimension)

In a material with a circular section with diameter D $\left(A = \frac{\pi D^2}{4}\right)$

$$\frac{dA}{A} = \frac{2dD}{D} = -\frac{2\nu\, d\ell}{\ell}$$

$$\frac{dR}{R} = \frac{d\ell}{\ell}(1+2\nu) + \frac{d\rho}{\rho}$$

Piezo-resistance fundamentals

$$\frac{dR}{R} = \frac{d\ell}{\ell}(1+2\nu) + \frac{d\rho}{\rho}$$

$$G = Gauge\ factor = \frac{dR/R}{d\ell/\ell} =$$

$$= \underbrace{1}_{\text{Var. of R due to var. of } \textbf{length}} + \underbrace{2\nu}_{\text{Var. of R due to var. of } \textbf{Area}} + \underbrace{\frac{d\rho/\rho}{d\ell/\ell}}_{\text{Var. of R due to the } \textbf{piezo-resistive effect}}$$

Piezoresistive effect= variation of resistivity ρ due to a mechanical stress.

Piezoresistivity in metals

In a metallic material, the piezoresistive effect (resistivity change due to a mechanical stress) is determined by the variation of the amplitude of the vibrations of the atoms constituting the material.

A longitudinal stress determines an increase of these vibrations, that in turn determines a reduction of electronic mobility, and therefore an increase in resistivity.

In **metals**, the percentage variations of resistivity and volume are proportional by Bridgman's constant C :

$$\frac{d\rho}{\rho} = C\frac{dV}{V}$$

(C=1.13÷1.15 in usual alloys, C=4.4 in platinum)

Piezoresistivity in metals

$$V = \frac{\pi \ell D^2}{4} \quad \Rightarrow \quad \frac{dV}{V} = \frac{d\ell}{\ell} + \frac{2dD}{D} = \frac{d\ell}{\ell}(1-2\nu)$$

Therefore, if the material isotropic, within the elastic limit, we have:

$$\frac{dR}{R} = \frac{d\ell}{\ell}\left[1+2\nu+C(1-2\nu)\right] = G\frac{d\ell}{\ell} = G\varepsilon$$

(G≈2, apart from platinum, where G≈6)

Therefore for small variations, the resistance is

$$R = R_0 + dR = R_0\left(1+\frac{dR}{R_0}\right) \cong R_0(1+G\varepsilon) = R_0(1+x)$$

where R_0 is the resistance when there is no applied stress, and $x=G\varepsilon$. Usually, $x<0.02$

Piezo-resistance in metals

Change in Resistance with Strain for Various Strain Gage Element Materials

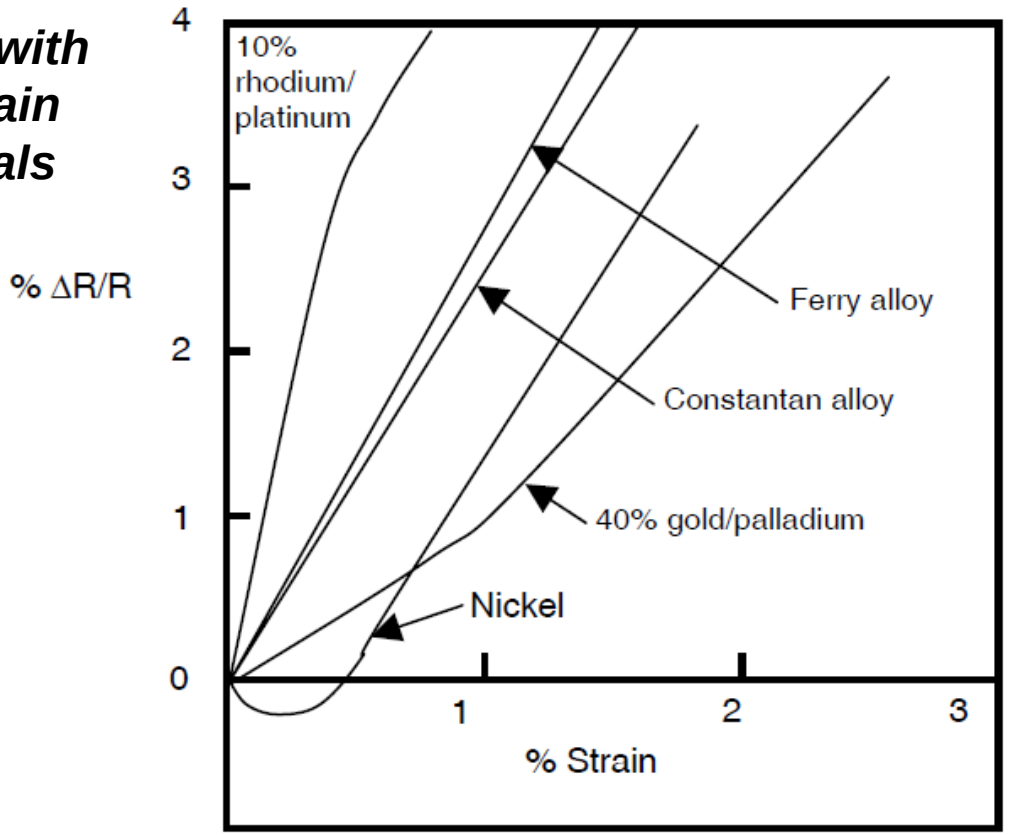

The Gage Factor is only of order unity and therefore the resistance changes in the gage is of the same order as the strain changes. In engineering materials this strain level is typically from 2 to 10,000 microstrain or 0.000002 to 0.01. Thus, changes in resistance in the gage of no more than 1% must be detected.

Numerical example

A 350 Ω strain gage having G=2.1 is attached to an aluminum strut (E=73 GPa). The outside diameter of the strut is 50 mm and the inside diameter is 47.5 mm. Calculate the change in resistance when the strut supports a 1000 kg load.

$$\Delta R = RG\varepsilon = RG\frac{F/A}{E}$$

From geometry, the area supporting the force is

$$A = \frac{\pi(D^2 - d^2)}{4} = \frac{\pi \times (97.5\ \text{mm}) \times (2.5\ \text{mm})}{4} = 191\ \text{mm}^2$$

Therefore, with R= 350 Ω, G=2.1, F=1000 kg =ˆ9800 N, and E = 73 GPa, we have

$$\Delta R = (350\ \Omega) \times 2.1 \times \frac{9800\ \text{N}}{(191 \times 10^{-6}\ \text{m}^2) \times 73\ \text{GPa}} = 0.52\ \Omega$$

which is less than 0.15% of the initial resistance.

Piezoresistivity in semiconductors

In **semiconductors**, submitted to applied stress, in addition to dimensional variations there is a change in the number of charge carrier and in their mobility.

Unlike metals, the resistivity change under stress dominates over the dimensional changes

The amplitude and the sign of the piezoresistive effect depend on :

1. material
2. charge carriers concentration
3. orientation of the crystallographic axes with respect to the applied stress

Piezoresistivity in semiconductors

Cubic structure and crystal planes of silicon

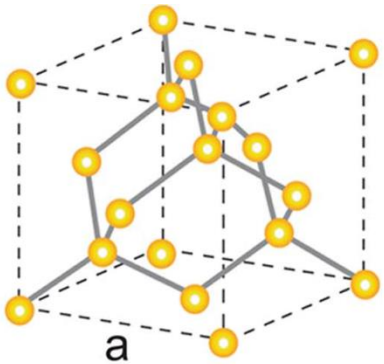

(a)

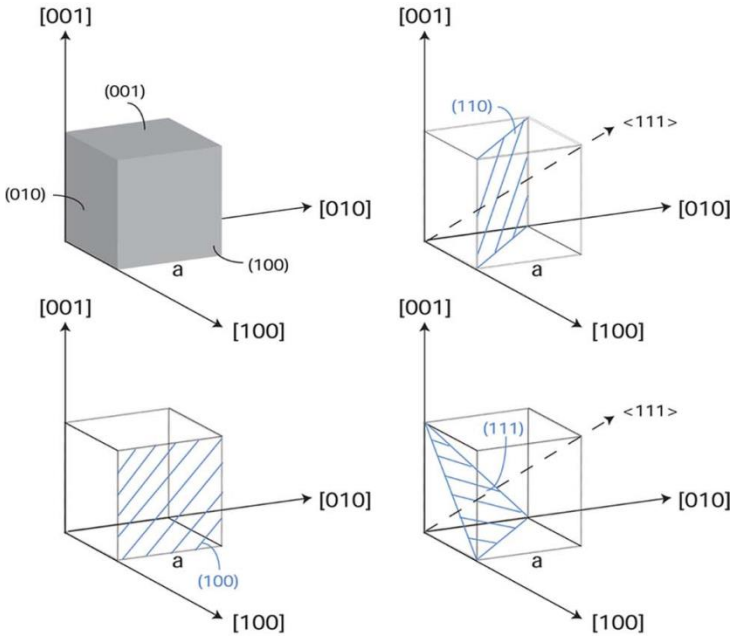

(b)

Components of stress on an infinitesimal unit element

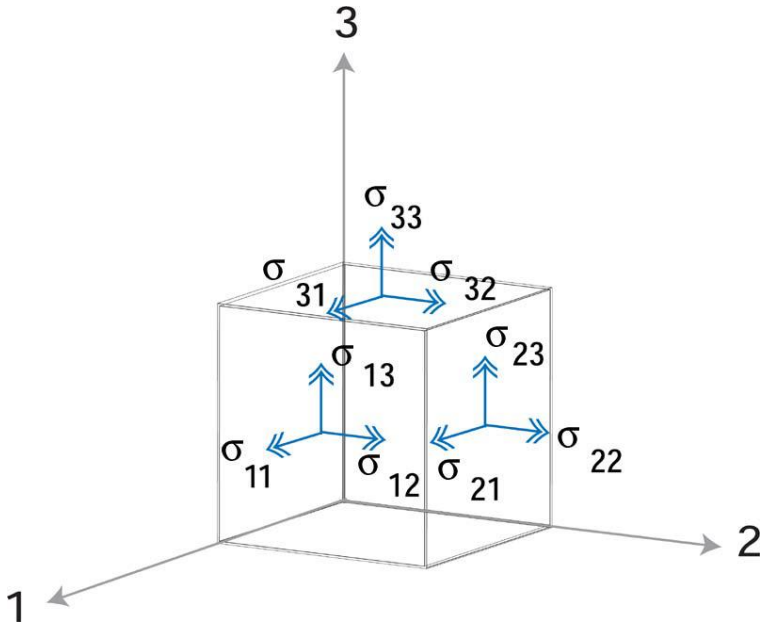

Piezoresistivity in semiconductors

To define the state of stress for a unit element, nine components, σij, must be specified:

$$\sigma = \begin{bmatrix} \sigma_{11} & \sigma_{12} & \sigma_{13} \\ \sigma_{21} & \sigma_{22} & \sigma_{23} \\ \sigma_{31} & \sigma_{32} & \sigma_{33} \end{bmatrix}$$

The first index i denotes the direction of the applied stress, while j indicates the direction of the force or stress. If i=j, the stress is normal to the specified surface, while i≠j indicates a shear stress on face i. From static equilibrium requirements that forces and moments sum to zero, a stress tensor is always symmetric, $\sigma_{ij} = \sigma_{ji}$, and thus the stress tensor contains only six independent components. Strain, ε_{ij}, is also directional.

The stress and strain are related by the elastic stiffness matrix C:

$$\begin{bmatrix} \sigma_{11} \\ \sigma_{22} \\ \sigma_{33} \\ \sigma_{23} \\ \sigma_{13} \\ \sigma_{12} \end{bmatrix} = \begin{bmatrix} c_{11} & c_{12} & c_{13} & c_{14} & c_{15} & c_{16} \\ c_{12} & c_{22} & c_{23} & c_{24} & c_{25} & c_{26} \\ c_{13} & c_{23} & c_{33} & c_{34} & c_{35} & c_{36} \\ c_{14} & c_{24} & c_{34} & c_{44} & c_{45} & c_{46} \\ c_{15} & c_{25} & c_{35} & c_{45} & c_{55} & c_{56} \\ c_{16} & c_{26} & c_{36} & c_{46} & c_{56} & c_{66} \end{bmatrix} \begin{bmatrix} \varepsilon_{11} \\ \varepsilon_{22} \\ \varepsilon_{33} \\ 2\varepsilon_{23} \\ 2\varepsilon_{13} \\ 2\varepsilon_{12} \end{bmatrix}$$

Piezoresistivity in semiconductors

The piezoresistive coefficients (π) require four subscripts because they relate two second-rank tensors of stress and resistivity. The first subscript refers to the electric field component (measured potential), the second to the current density (current), and the third and fourth to the stress (stress has two directional components).

For conciseness, the subscripts of each tensor are also collapsed, e.g., $\pi_{1111} \rightarrow \pi_{11}$, $\pi_{1122} \rightarrow \pi_{12}$, $\pi_{2323} \rightarrow \pi_{44}$.

These relations have been generalized for a fixed voltage and current orientation (ω) as a function of stress (λ):

$$\frac{\Delta\rho_\omega}{\rho} = \sum_{\lambda=1}^{6} \pi_{\omega\lambda}\sigma_\lambda$$

Piezoresistivity in semiconductors

For a simple tension or compression, if electrons flow along the direction of the stress, the relative variation of resistivity is proportional to the applied stress:

$$\frac{d\rho}{\rho_0} = \pi_L \sigma$$

where π_L represents the piezo-resistive longitudinal coefficient and ρ_0 the resistivity of the material at rest. The gauge factor is

$$G = \frac{\Delta R / R_0}{\varepsilon} = 50 \div 200$$

Semiconductors with a low number of charge carriers show high values of G, but are highly sensible to temperature and show non linear characteristic and vice versa.

Piezoresistive effect: semiconductors

The relationships that better describe dR=f(ε) are:

for a p-type material:

$$\frac{dR}{R} = K_1\varepsilon + K_2\varepsilon^2$$

for a n-type material:

$$\frac{dR}{R} = -K_3\varepsilon + K_4\varepsilon^2$$

Effect of temperature

- influences the resistivity (especially in semiconductors);
- influences the dimensions (in metals, until 50 με/°C) of both sensing and support material;
- changes with current that is necessary to measure resistance variations
- thermoelectric effects at the junctions of different metals

Metals vs semiconductors

Table 9.2. Characteristics of Some Resistance Strain Gauges

Material	Gauge factor (S_e)	Resistance, Ω	Temperature coefficient of resistance ($°C^{-1} \times 10^{-6}$)	Notes
57% Cu–43%Ni	2.0	100	10.8	S_e is constant over a wide range of strain; for use under 260°C
Platinum alloys	4.0–6.0	50	2,160	For high-temperature use
Silicon	−100 to +150	200	90,000	High sensitivity, good for large strain measurements

TABLE 2.2 Typical Characteristics of Metal and Semiconductor Strain Gages

Parameter	Metal	Semiconductor
Measurement range	0.1 to 40,000 $\mu\varepsilon$	0.001 to 3000 $\mu\varepsilon$
Gage factor	1.8 to 2.35	50 to 200
Resistance, Ω	120, 350, 600, . . . , 5000	1000 to 5000
Resistance tolerance	0.1% to 0.2%	1% to 2%
Size, mm	0.4 to 150 Standard: 3 to 6	1 to 5

1) the applied stress should not exceed the elastic limit of the gage. Strain should not exceed 4% of gage length and ranges, approximately, from 3000 με for semiconductor gages to 50,000 με for metal gages.

2) the measurement will be correct only if all the stress is transmitted to the gage. This is achieved by carefully bonding the gage with an elastic adhesive that must be also stable with time and temperature. At the same time, the gage must be electrically insulated from the object it adheres to and be protected from the environment.

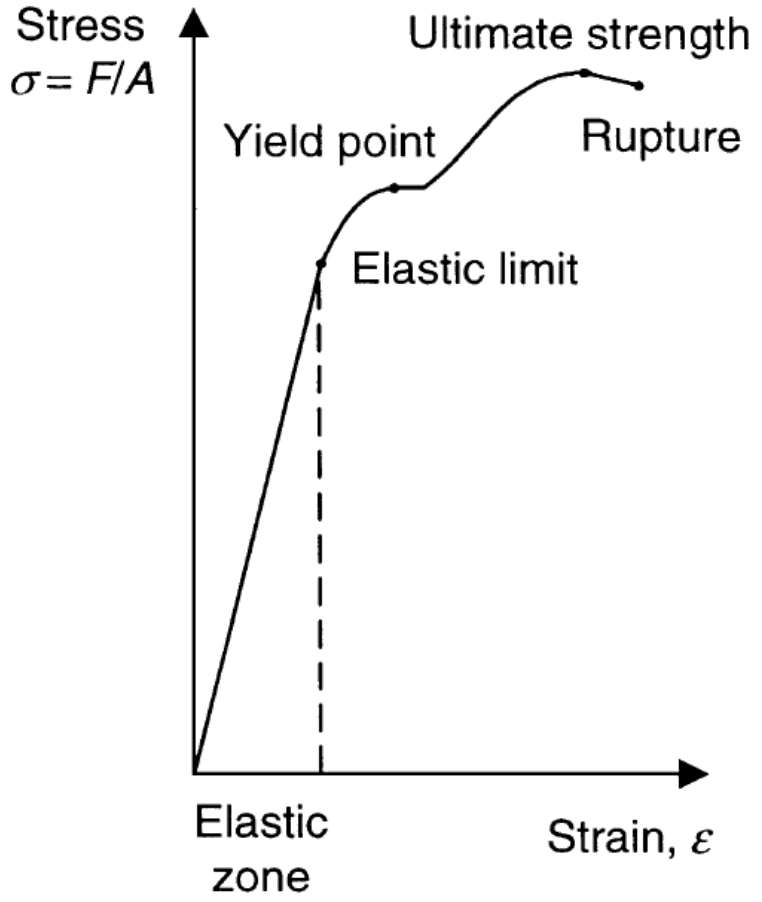

Stress-strain diagram for mild steel.
The elastic region has been greatly enlarged.

It is assumed that all strains are in the same plane; that is, there is no stress in any direction perpendicular to the gage wires. To have a significant electric resistance for metal gages, they consist of a grid containing several longitudinal segments connected by shorter transverse segments having a larger cross section.
Thus the transverse sensitivity is only from 1% to 2% of the longitudinal sensitivity.

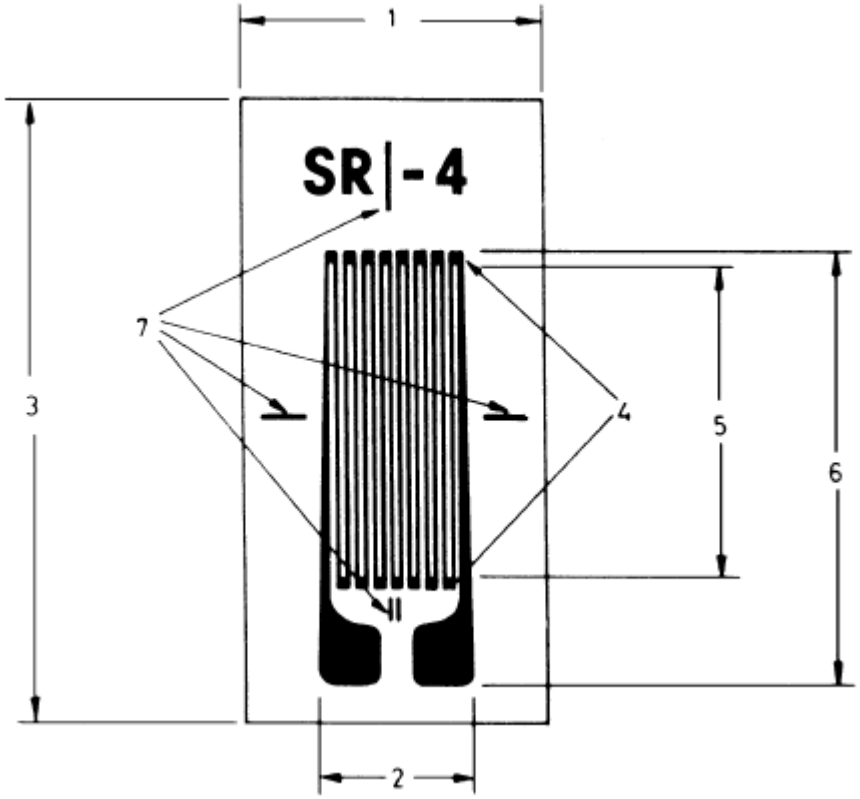

Parameters for a foil strain gage (from BLH Electronics): 1, matrix width; 2, grid width; 3, matrix length (carrier); 4, end loops; 5, active grid length; 6, overall gage length; 7, alignment marks. Typical thicknesses are 3.8 mm and 5 mm, depending on material type.

Adhesive Strain gauges

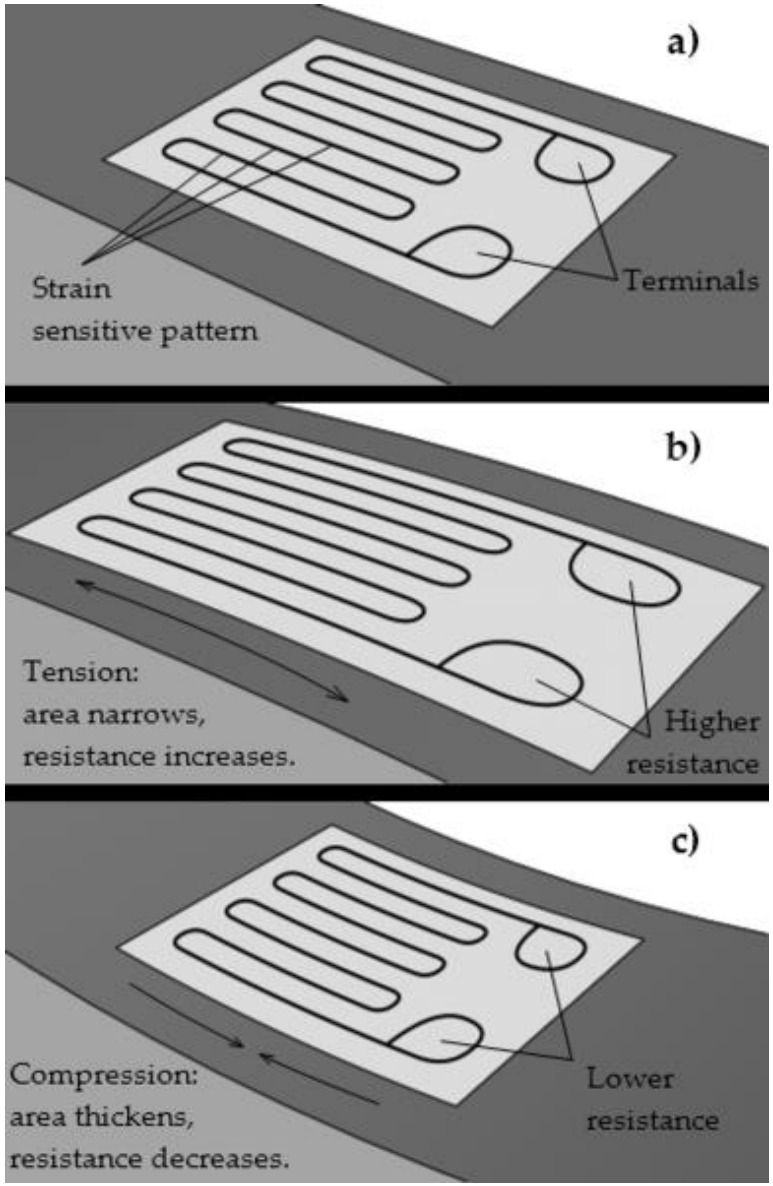

Adhesive Strain gauges

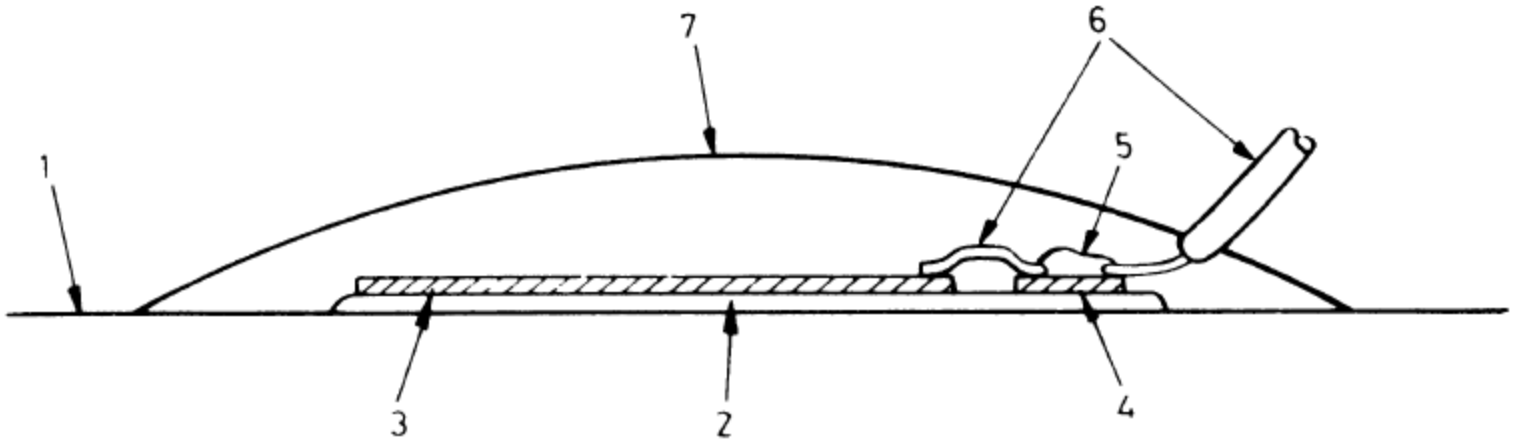

Installation of a foil strain gage (from BLH Electronics): 1, substrate material; 2, adhesive; 3, strain gage; 4, solder terminals; 5, solder; 6, lead wires; 7, environmental barrier.

Adhesive Strain gauges

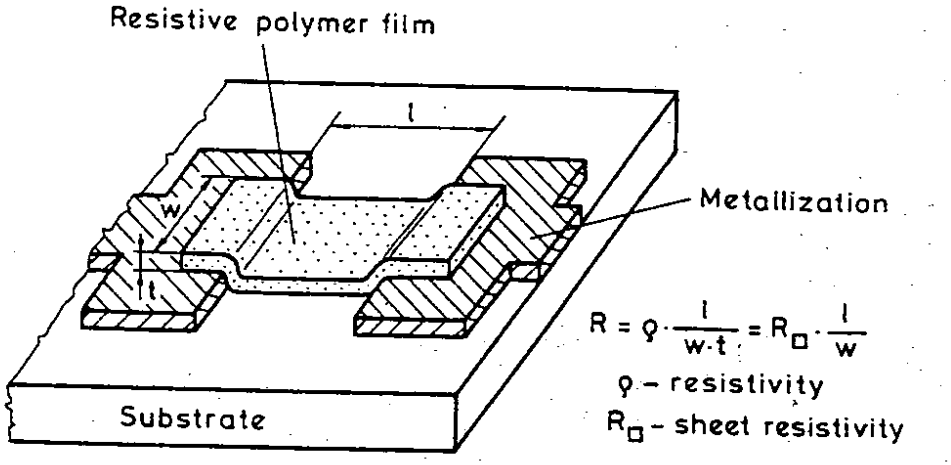

3.1(b)

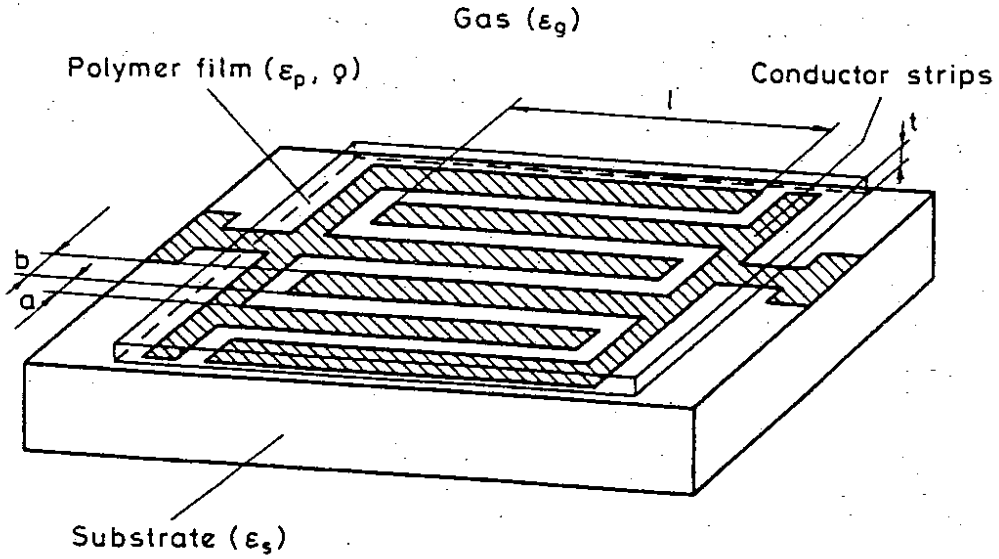

Adhesive Strain gauges

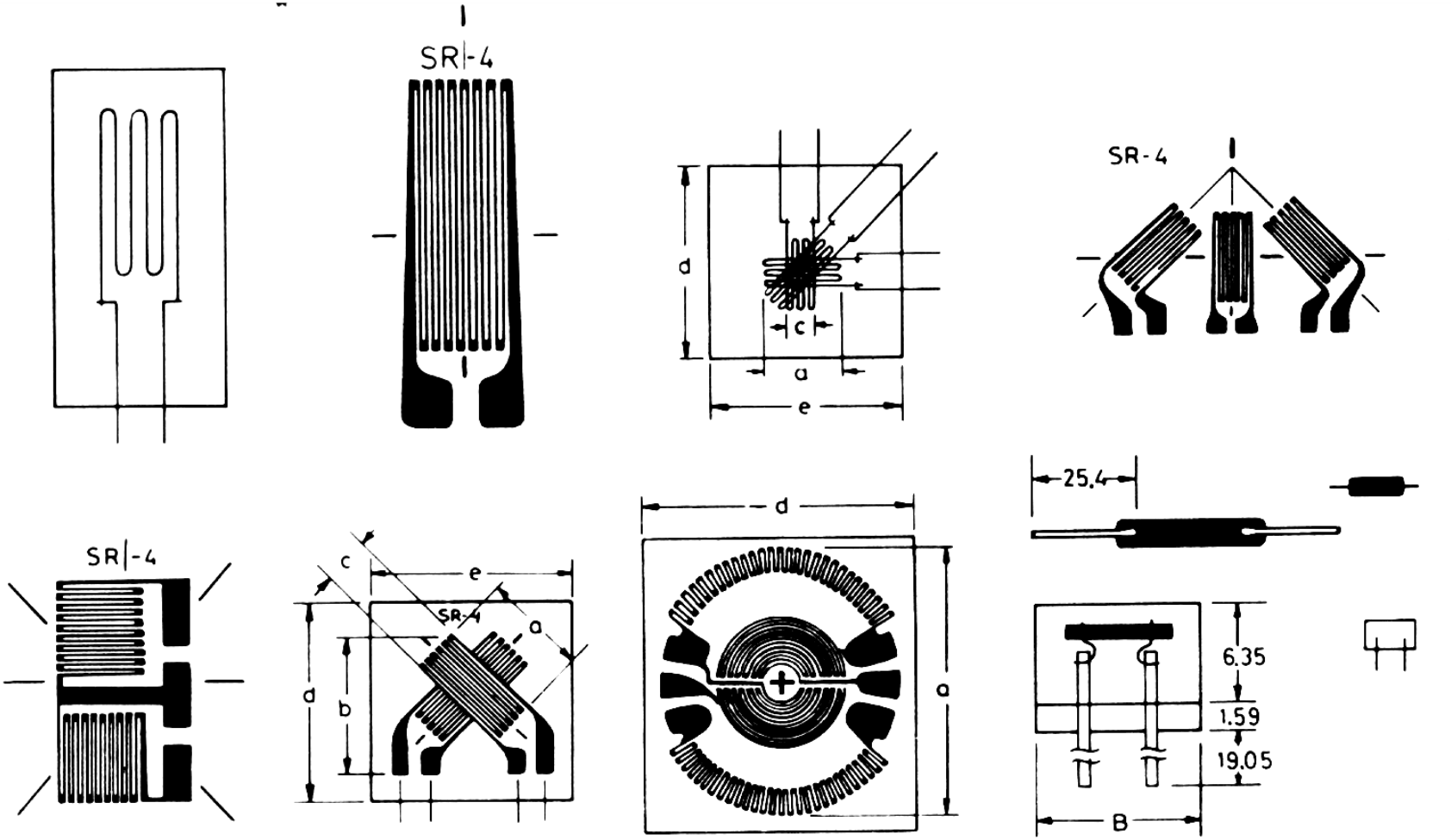

FIGURE 2.7 Several bonded and unbonded metal and semiconductor strain gages (from BLH Electronics).

Strain gauges: effect of temperature

Temperature interferes through several mechanisms.
It affects the resistivity of the material, its dimensions, and the dimensions and Young's modulus of the support material.
Thus once the gage is cemented, any change in temperature yields a change in resistance, hence an apparent strain, even before applying any mechanical force.
In metal strain gages this change can be as large as 50 με/°C.
Temperature interference may be compensated by dummy gages implementing the opposing-inputs method. Dummy gages are equal to the sensing gages and placed near them in order to experience the same temperature change but without experiencing any mechanical effort.

Strain gauges: effect of temperature

Temperature interference is stronger in semiconductor strain gages. In self temperature-compensated gages, the increase in resistivity with increasing temperature is compensated by a decrease in resistance due to the expansion of the backing material. This method achieves thermal-induced apparent strain of only 5 με/°C over a temperature range of 20°C.

Strain-gage resistance measurement implies passing an electric current through it, which causes heating. The maximal current is 25 mA for metal gages if the base material is a good heat conductor (steel, copper, aluminum, magnesium, titanium) and is 5 mA if it is a poor heat conductor (plastic, quartz, wood). The permissible power increases with the gage area and ranges from 770 mW/cm^2 to 150 mW/cm^2, depending on the backing. Maximal power dissipation in semiconductor strain gages is 250 mW.

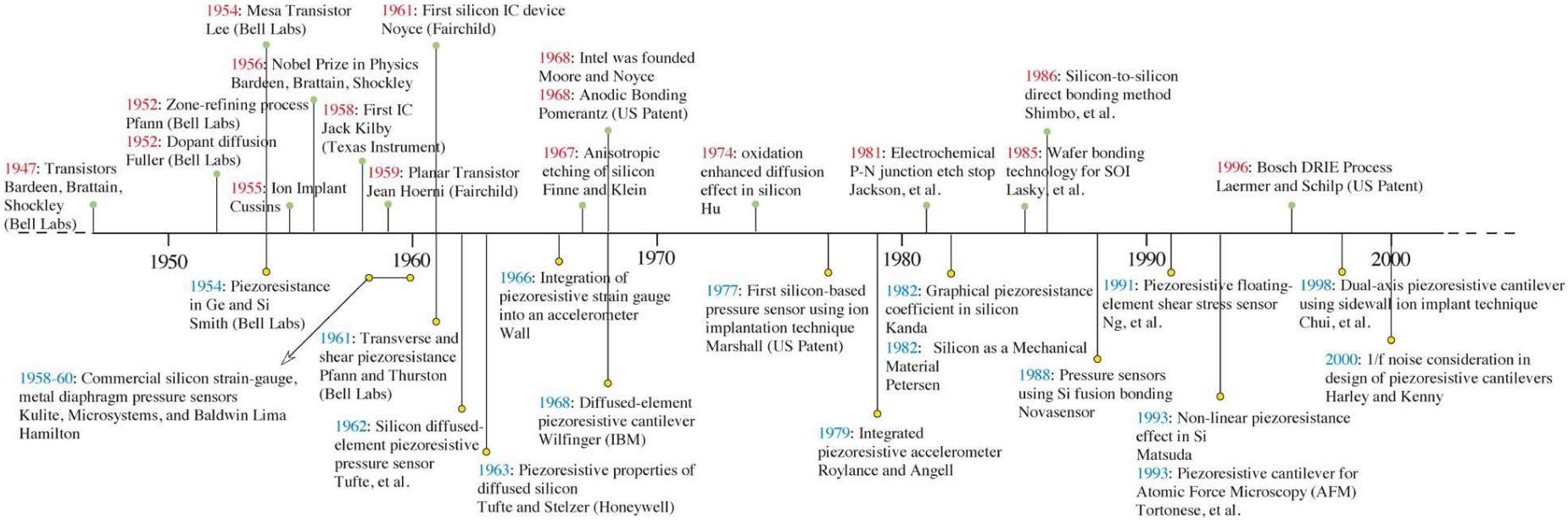
1947: Transistors
Bardeen, Brattain, Shockley
(Bell Labs)
1950
1952: Zone-refining process
Pfann (Bell Labs)
1952: Dopant diffusion
Fuller (Bell Labs)
1954: Mesa Transistor
Lee (Bell Labs)
1954: Piezoresistance in Ge and Si
Smith (Bell Labs)
1955: Ion Implant
Cussins
1956: Nobel Prize in Physics
Bardeen, Brattain, Shockley
1958: First IC
Jack Kilby
(Texas Instrument)
1958-60: Commercial silicon strain-gauge, metal diaphragm pressure sensors
Kulite, Microsystems, and Baldwin Lima Hamilton
1959: Planar Transistor
Jean Hoerni (Fairchild)
1960
1961: First silicon IC device
Noyce (Fairchild)
1961: Transverse and shear piezoresistance
Pfann and Thurston
(Bell Labs)
1962: Silicon diffused-element piezoresistive pressure sensor
Tufte, et al.
1963: Piezoresistive properties of diffused silicon
Tufte and Stelzer (Honeywell)
1966: Integration of piezoresistive strain gauge into an accelerometer
Wall
1967: Anisotropic etching of silicon
Finne and Klein
1968: Intel was founded
Moore and Noyce
1968: Anodic Bonding
Pomerantz (US Patent)
1968: Diffused-element piezoresistive cantilever
Wilfinger (IBM)
1970
1974: oxidation enhanced diffusion effect in silicon
Hu
1977: First silicon-based pressure sensor using ion implantation technique
Marshall (US Patent)
1979: Integrated piezoresistive accelerometer
Roylance and Angell
1980
1981: Electrochemical P-N junction etch stop
Jackson, et al.
1982: Graphical piezoresistance coefficient in silicon
Kanda
1982: Silicon as a Mechanical Material
Petersen
1985: Wafer bonding technology for SOI
Lasky, et al.
1986: Silicon-to-silicon direct bonding method
Shimbo, et al.
1988: Pressure sensors using Si fusion bonding
Novasensor
1990
1991: Piezoresistive floating-element shear stress sensor
Ng, et al.
1993: Non-linear piezoresistance effect in Si
Matsuda
1993: Piezoresistive cantilever for Atomic Force Microscopy (AFM)
Tortonese, et al.
1996: Bosch DRIE Process
Laermer and Schilp (US Patent)
1998: Dual-axis piezoresistive cantilever using sidewall ion implant technique
Chui, et al.
2000
2000: 1/f noise consideration in design of piezoresistive cantilevers
Harley and Kenny

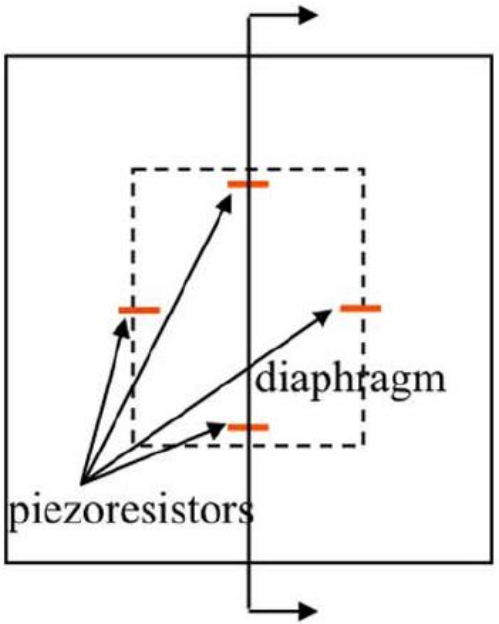

(a)

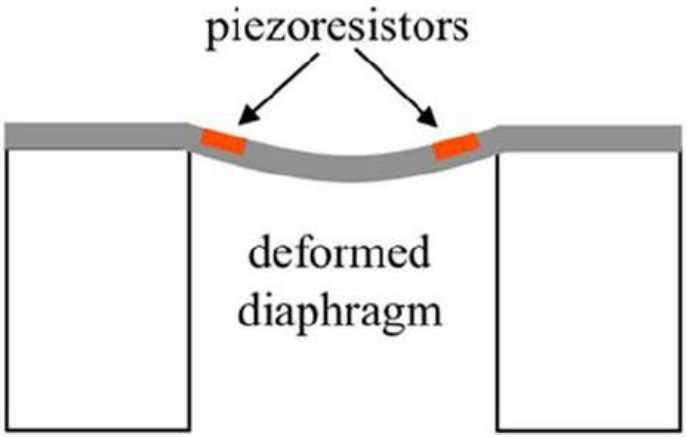

(b)

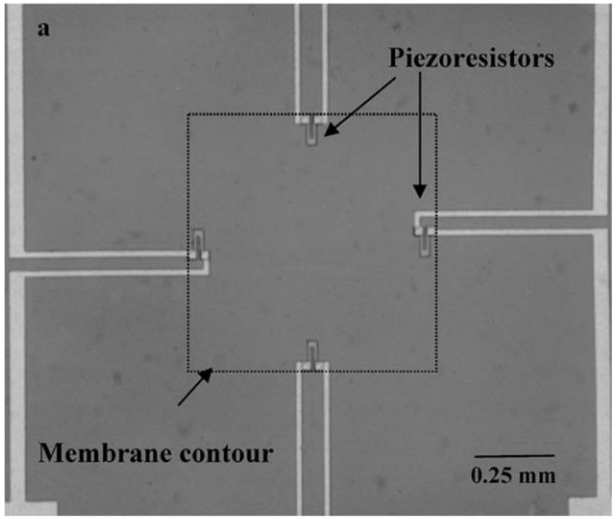

(c)

Illustration of a piezoresistive pressure sensor.

(a) Top view of piezoresistive pressure sensor. Four piezoresistors are placed on each edge forming a Wheatstone bridge circuit.

(b) Cross section A-A showing deflected diaphragm with piezoresistors at maximum stress locations.

(c) Photograph of a pressure sensors with four 3C-SiC (a polytype of silicon carbide, see Section IV-A) piezoresistors.

Pressure sensor (Radi Medical Systems AB)

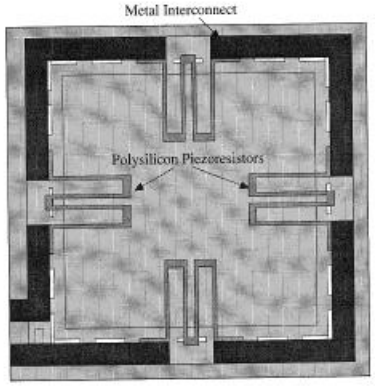

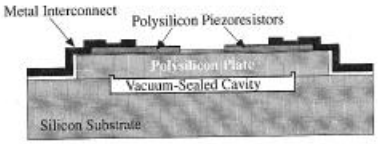

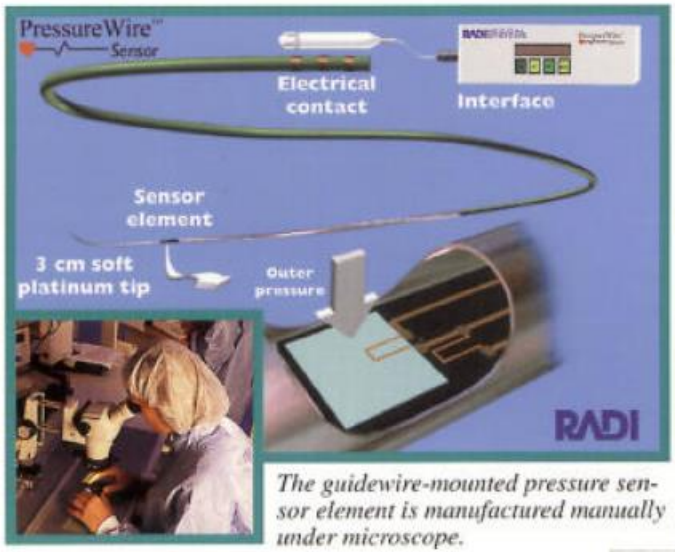

The guidewire-mounted pressure sensor element is manufactured manually under microscope.

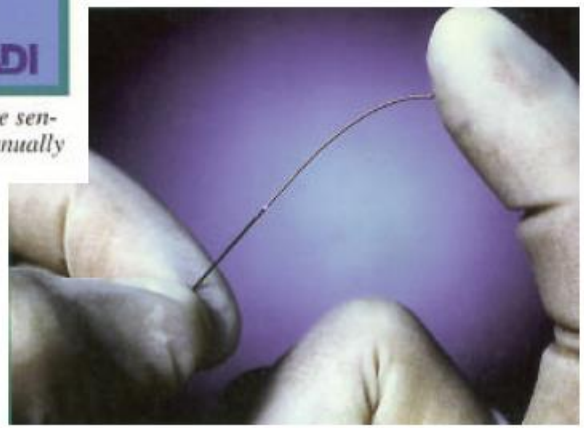

Example: pressure transducer

Scale: 1 cm
½ inch

FEATURES

- 0...1 psi to 0...150 psi
- Precision temperature compensation
- Calibrated zero and span
- Small size
- Low noise
- High accuracy
- High impedance for low power applications

APPLICATIONS

- Medical equipment
- Barometry
- Computer peripherals
- Pneumatic control

Piezoresistive pressure sensors

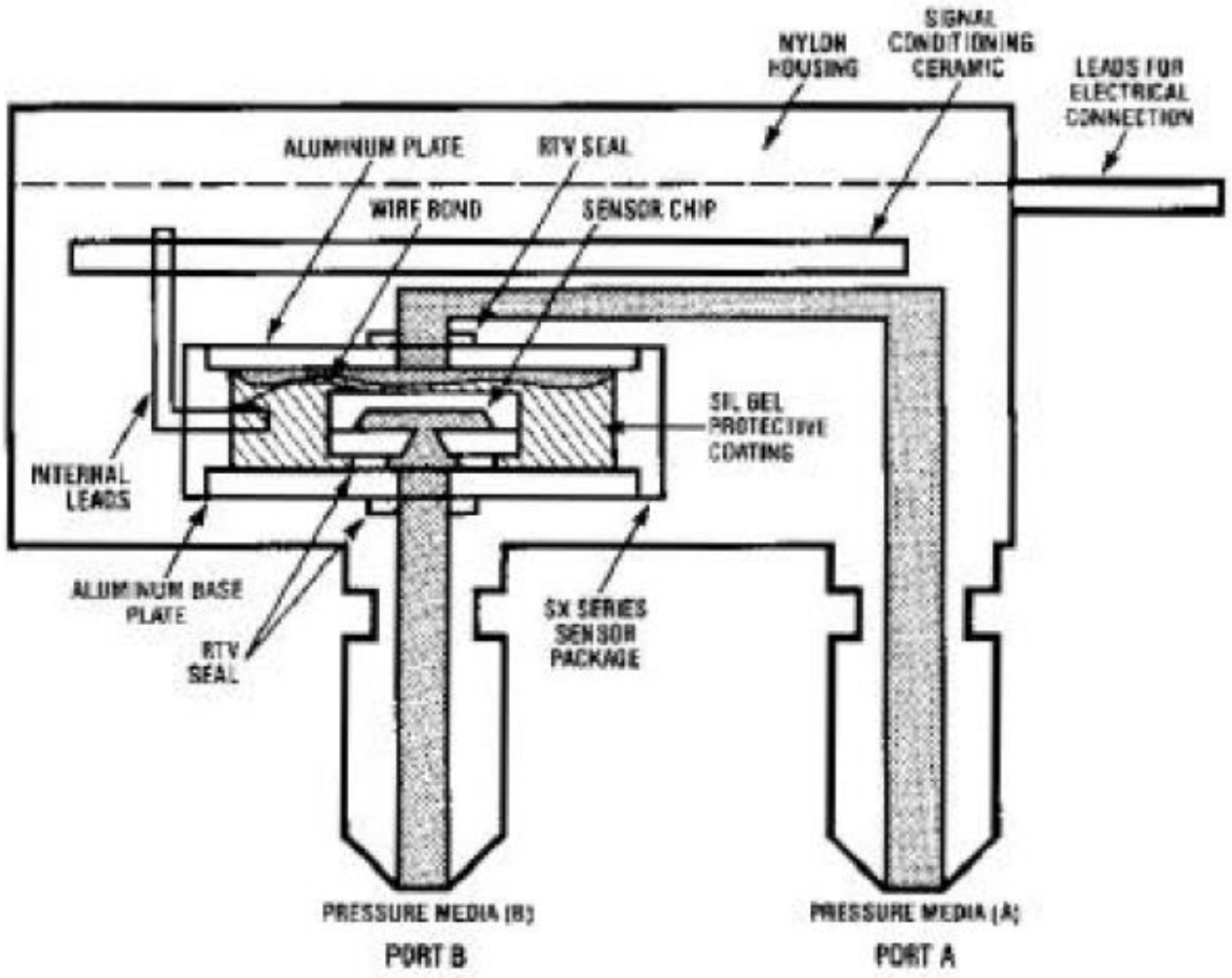

Physical construction (cutaway diagram) (not drawn to scale)

Piezoresistive pressure sensors

The sensor is obtained by anisotropic etching of silicon wafer to create circular or square holes ending very close to the upper surface.

In this way silicon diaphragms of area 7 x 7mm, thickness 5- 50±1 μm are created

Size and thickness of the diaphragm depend on the range of pressures that must be measured.

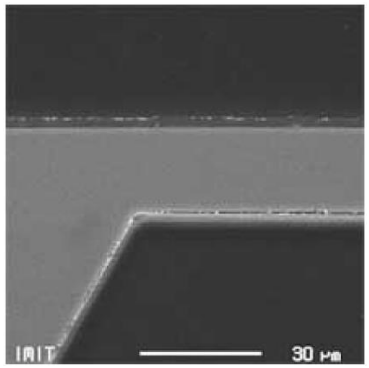

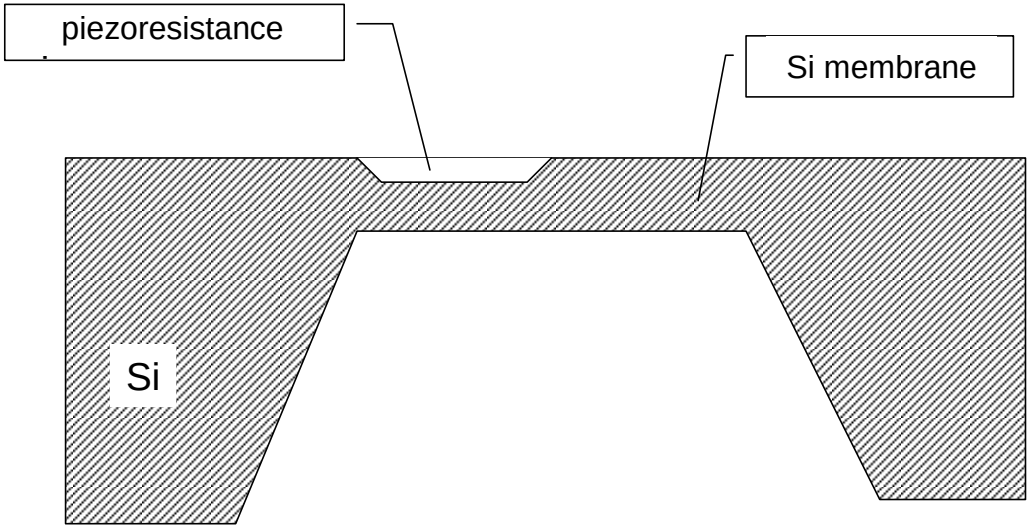

EQUIVALENT CIRCUIT

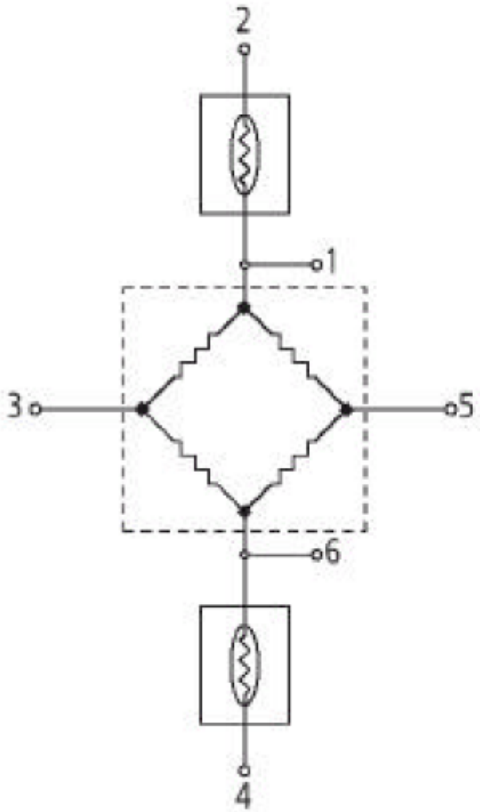

ELECTRICAL CONNECTION

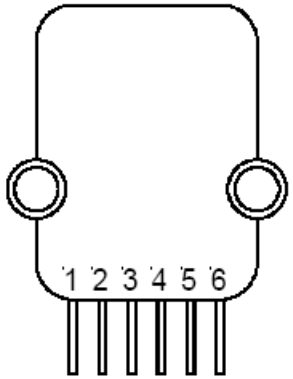

Bottom view

Pin 1) Temperature output (+)
Pin 2) V_S
Pin 3) Output (+)
Pin 4) Ground
Pin 5) Output (-)
Pin 6) Temperature output (-)

Note: The polarity indicated is for pressure applied to port B (for absolute devices pressure is applied to port A and the output polarity is reversed.)

Evolution of micromachined pressure sensors

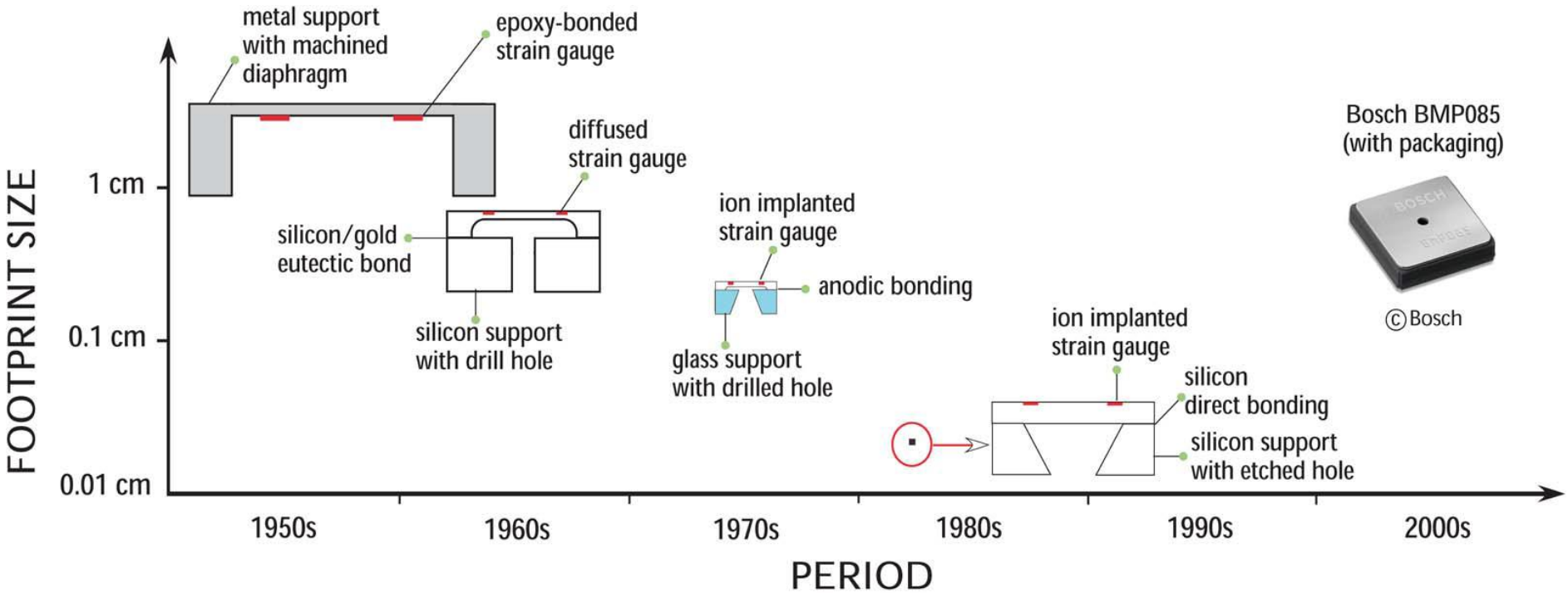

The SP80 is an example of **piezoresistive integrated pressure** sensor with the pressure-sensitive diaphragm micromachined in a silicon chip by anisotropic etching and with ion implanted piezoresistors in a full Wheatstone bridge configuration as the electronic sensing element. In addition, a temperature measuring resistor and a heating resistor are implanted on the same chip, making it possible to thermostat the chip to minimise thermal drifts. By varying the area and the thickness of the diaphragm, the family of these sensors comprises a number of pressure ranges from 0.5 Bar full scale pressure up to 60 Bar full scale pressure, all with equally high full scale output signal.

Piezoresistive pressure sensors Fabrication (1/2)

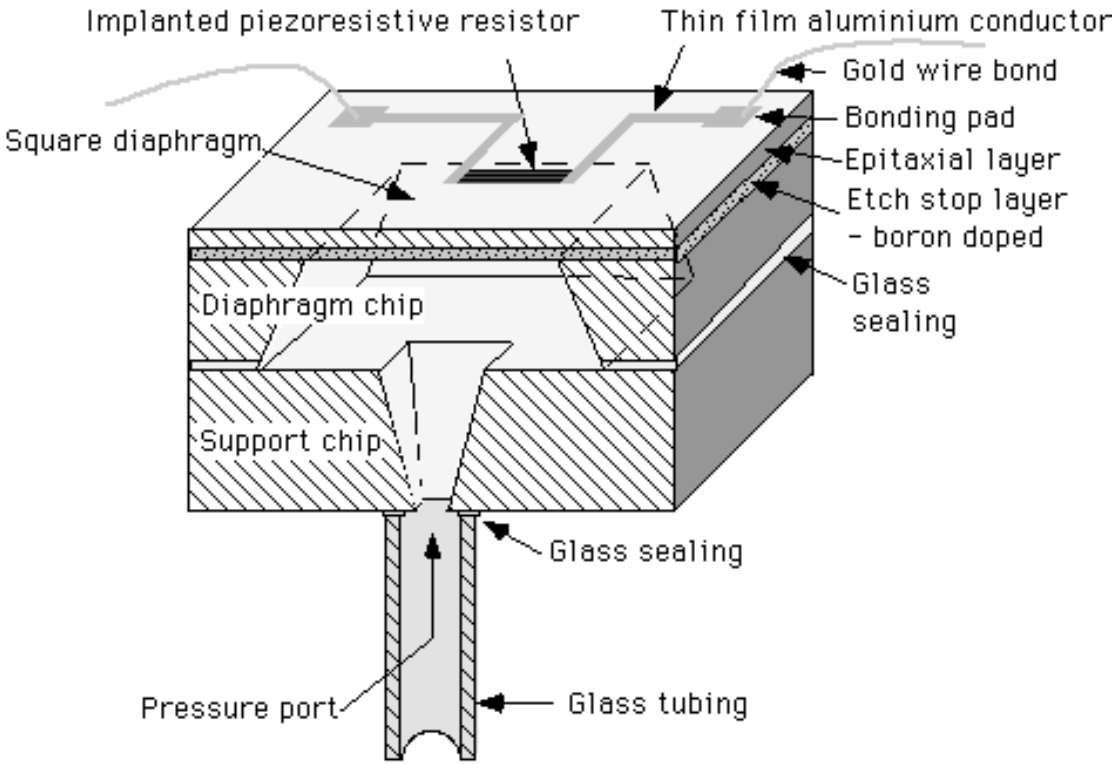

The size of the chips is 4*4 mm, chip thickness approximately 0.3 mm, the diaphragm area is typical 2*2 mm and the diaphragm thickness is typical 30μm.

The diaphragm is manufactured by stripping off the surface oxide of the silicon wafer by means of photolithographic technique in the areas we want the diaphragm cavity. Then the wafer is etched in an anisotropic etching solution with the remaining oxide as masking film.

Piezoresistive pressure sensors Fabrication (2/2)

This etching solution attacks the single crystal silicon with different speed in the different crystal directions. The etch is extremely slow in the <1-1-1> direction, meaning that the etch is stopped towards the (1-1-1) planes. The chip material is (1-0-0) silicon, and this means that the etch cavity is surrounded by four (1-1-1) planes which have an angle of inclination of 54.7 degrees relative to the (1-0-0) surface plane, rendering a cavity with four sloped walls.

In this way we can control the diaphragm area, but we also need a technique to control the thickness of the diaphragm, and in this design this is done by doping the silicon with a high concentration boron stopping layer. The etching speed is slowed considerately with increased boron concentration, thereby making it possible to remove the wafer from the etching solution when the slow-etching mode is reached and a well-defined diaphragm thickness is obtained.

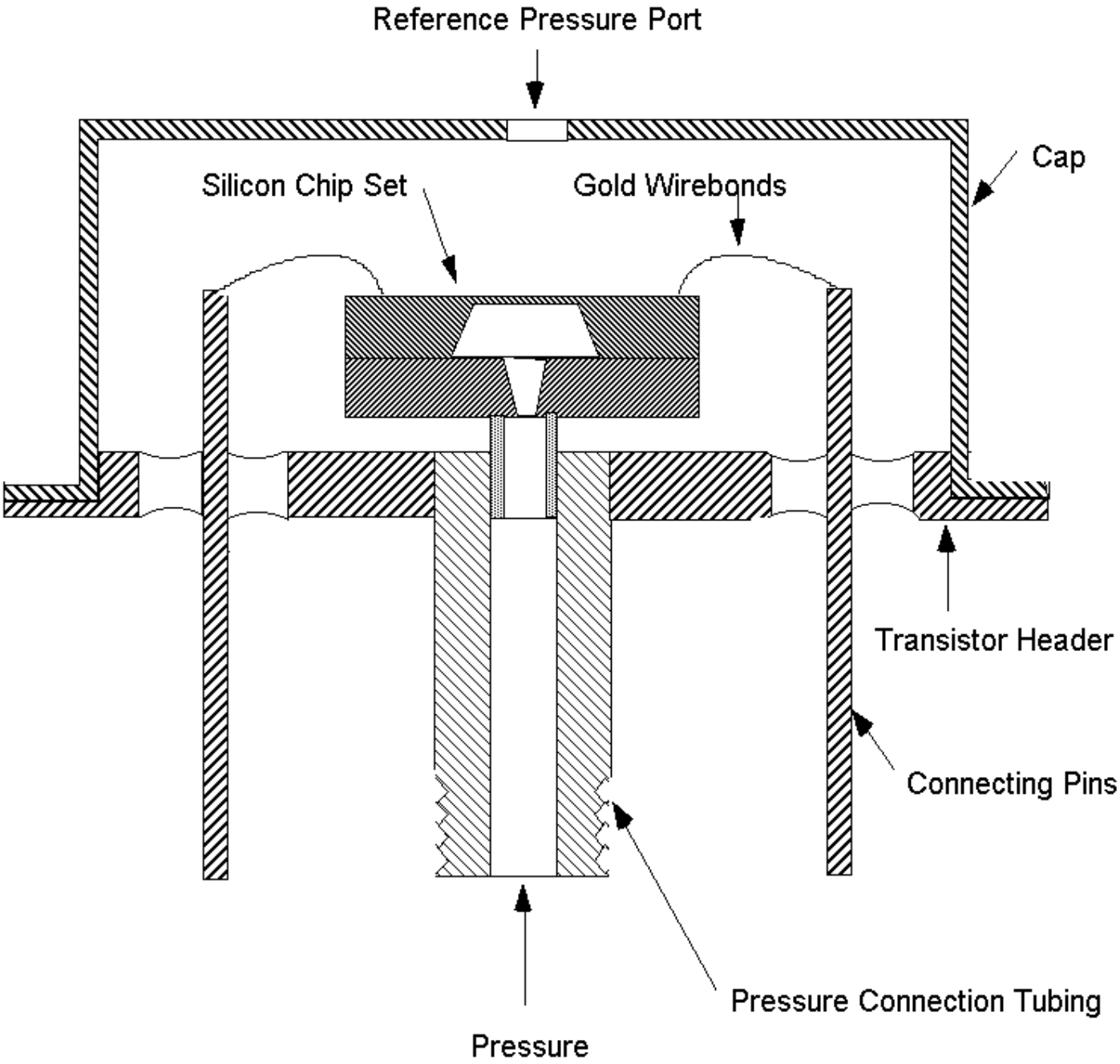
Reference Pressure Port
Cap
Silicon Chip Set
Gold Wirebonds
Transistor Header
Connecting Pins
Pressure Connection Tubing
Pressure

Atomic force microscopy (AFM)

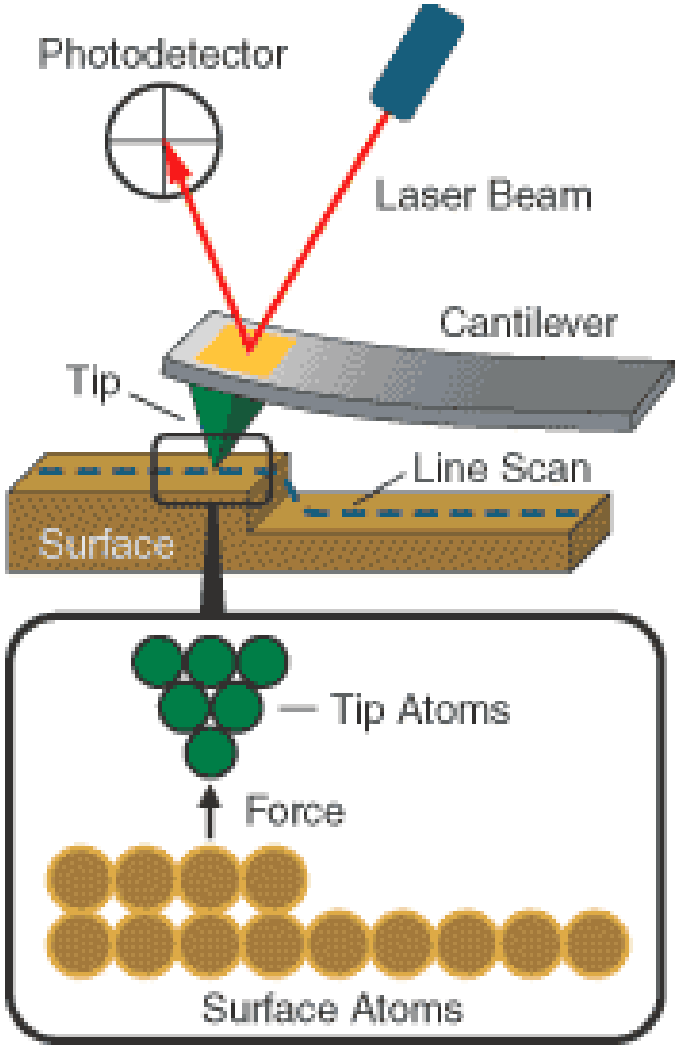

http://www.molec.com/what_is_afm.html

- Invented in 1986
- Cantilever
- Tip
- Surface
- Laser
- Multi-segment photodetector

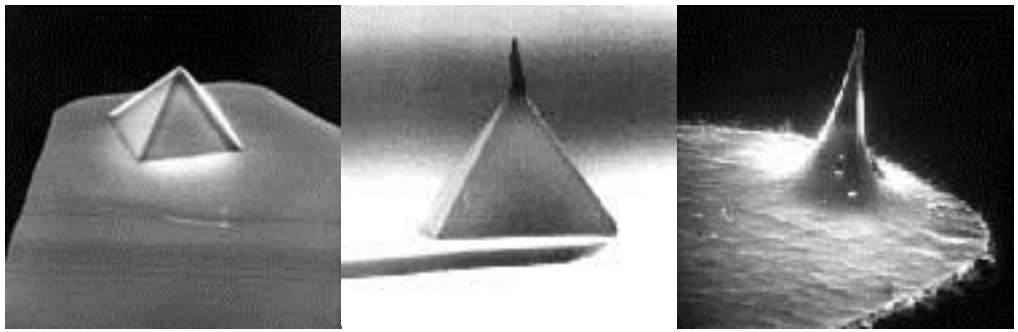

Three common types of AFM tip. (a) normal tip (3 μm tall); (b) supertip; (c) Ultralever (also 3 μm tall).

Electron micrographs by Jean-Paul Revel, Caltech. Tips from Park Scientific Instruments; supertip made by Jean-Paul Revel.

http://stm2.nrl.navy.mil/how-afm/how-afm.html#imaging%20modes

Dual axis Atomic Force Microscopy (AFM) cantilever

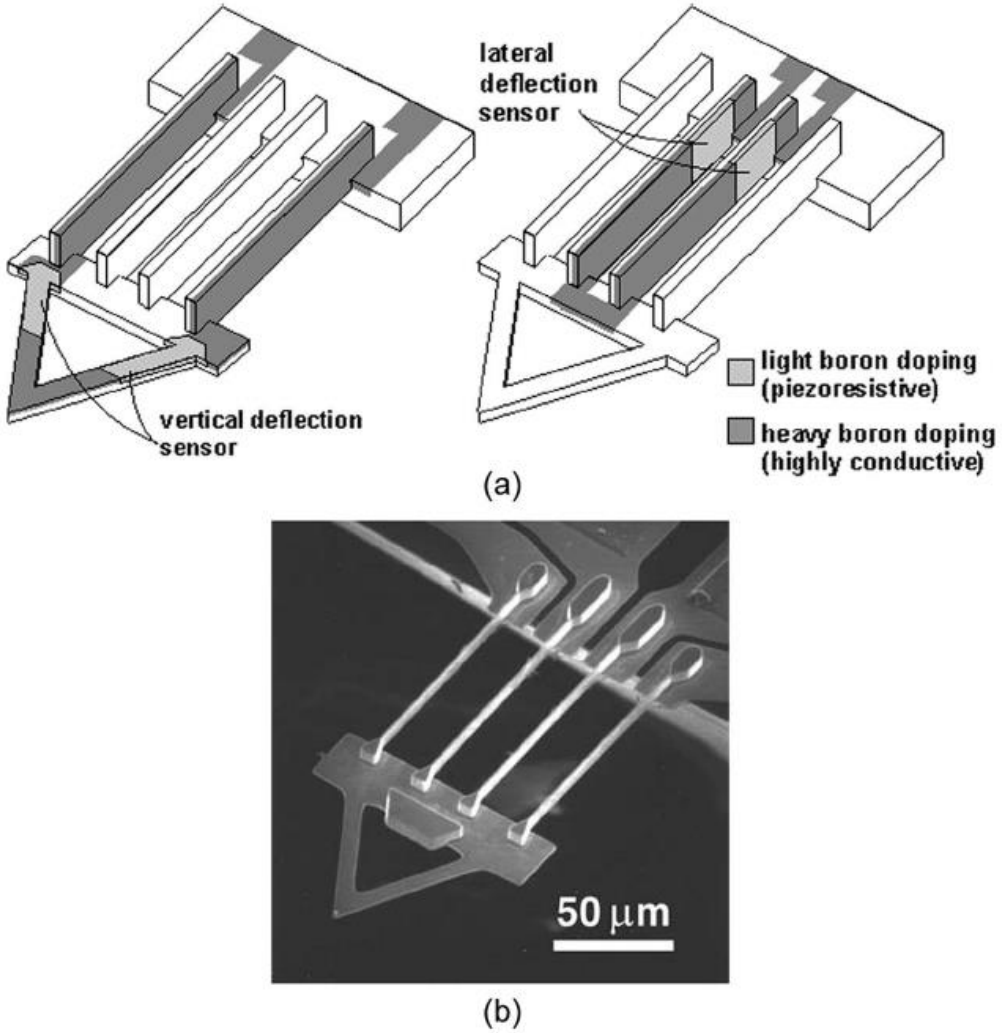

Fig. 21. *(a) Dual-axis AFM cantilever with orthogonal axes of compliance. Oblique ion implants are used to form electrical elements on vertical sidewalls and horizontal surfaces simultaneously. (b) SEM Image of a dual-axis AFM cantilever. Reprinted with permission from Chui et al. [122]. © 1998 American Institute of Physics.*

Light dependent resistors (LDR)

Light-dependent resistors (LDRs) - photoresistors, photoconductors - rely on the variation in electric resistance in a semiconductor caused by the incidence of optical radiation (electromagnetic radiation with wavelength from 1 mm to 10 nm)

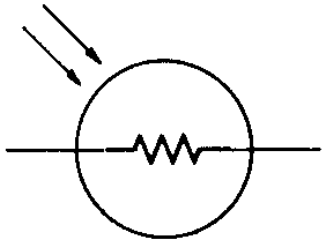

The electrical conductivity of a material depends on the number of charge carriers in the conduction band.

Most of the electrons in a semiconductor at ambient temperature are in the valence band. Thus it behaves like an electrical insulator. But when its temperature rises, electron vibrations increase; and because valence and conduction bands are very close in semiconductors, there is an increasing number of electrons raised from the valence band to the conduction band, thus increasing the conductivity.

In a doped semiconductor, this raising of electrons is even easier because, in addition to band-to-band transitions, a donor atom can be ionized, thus contributing an electron to the conduction band, or an acceptor atom can be ionized, thus leaving behind a hole in the valence band.

The sensitivity to incident radiation depends on how long these carriers remain free before recombining.

The energy needed to raise electrons from the valence to the conduction band can be provided by external energy sources other than heat - for example, by optical radiation or by an electric voltage.
The energy E and frequency f of optical radiation are related by

$$E = h \cdot f$$

where $h = 6.62 \cdot 10^{-34}$ J·s is Planck's constant.

If the incident radiation has enough energy to excite the electrons from one band to another, but without exceeding the threshold for them to leave the material, there is an **internal photoelectric effect**; and the greater the illumination (incident power per unit surface area), the higher the conductivity.

If that threshold were exceeded, there would be an **external photoelectric effect**. In conductors, the conductivity by itself is so high that the change produced by the incident radiation is not noticeable.

Light dependent resistor (LDR)

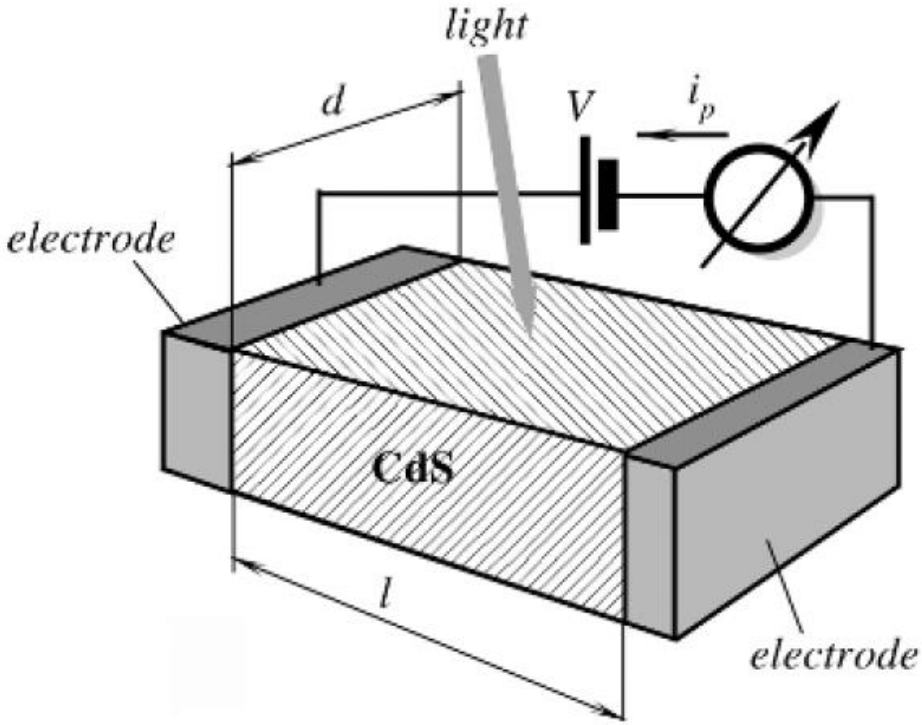

(A)

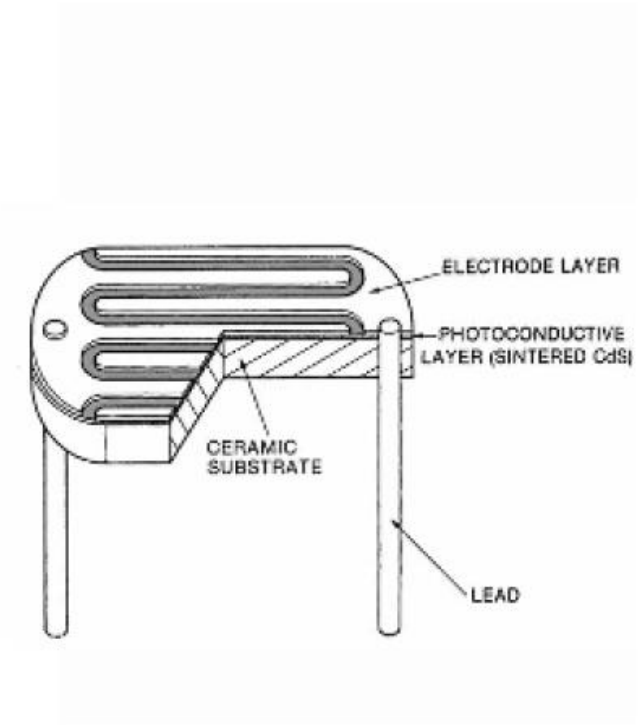

(B)

Fig. 14.14. Structure of a photoresistor (A) and a plastic-coated photoresistor having a serpentine shape (B).

Electromagnetic spectrum: electromagnetic radiation energy

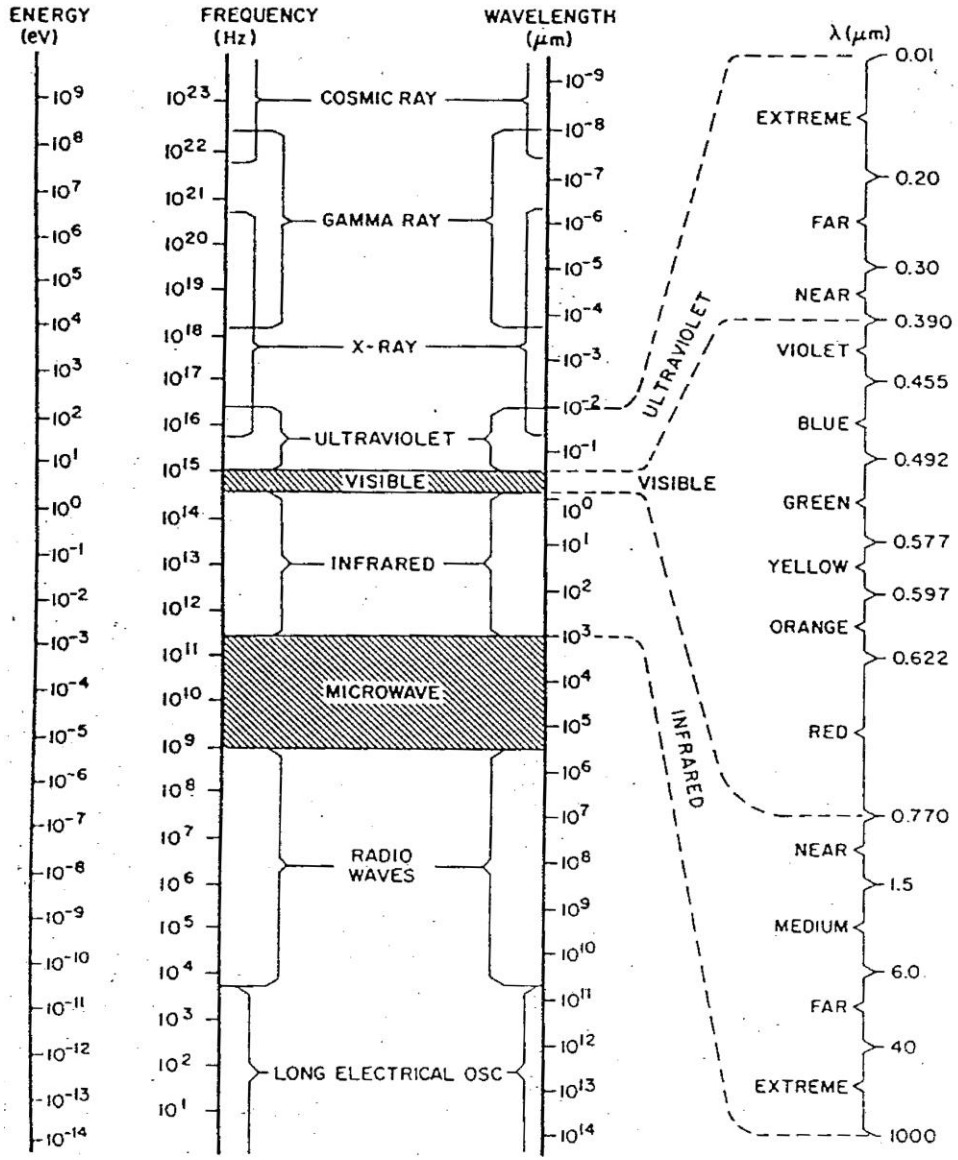

Internal photoelectric effect

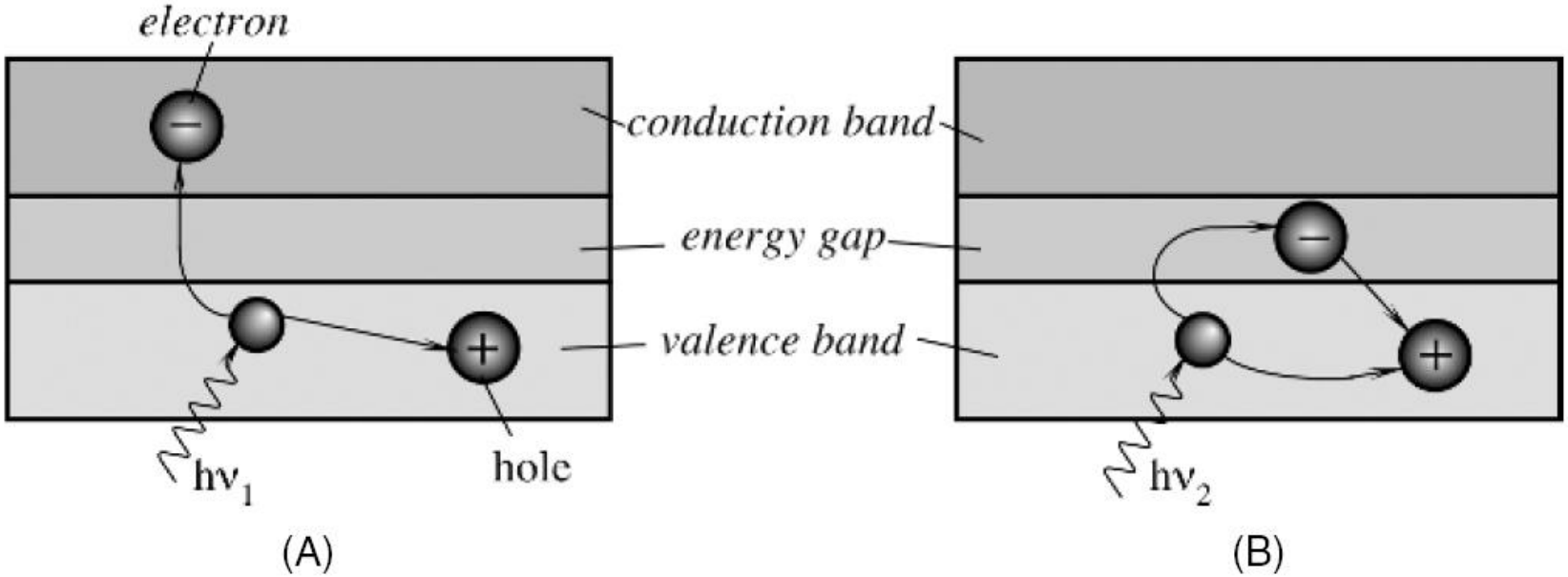

Fig. 14.1. Photoeffect in a semiconductor for high-energy (A) and low-energy (B) photons.

$$\lambda = hc/E$$

if E is expressed in eV (1 eV = 1.602 x 10^{-19} J),

$$\lambda\,(\mu m) = 1.24 / E(eV)$$

TABLE 2.6 Band Gap (in electron-volts) and Maximal Wavelength (in micrometers) for Various Intrinsic Semiconductors [10]

Material	Band Gap (eV)	Maximal Wavelength (μm)
ZnS	3.60	0.345
CdS	2.40	0.52
CdSe	1.80	0.69
CdTe	1.50	0.83
Si	1.12	1.10
Ge	0.67	1.85
PbS	0.37	3.35
InAs	0.35	3.54
Te	0.33	3.75
PbTe	0.30	4.13
PbSe	0.27	4.58
InSb	0.18	6.90

Light dependent resistor (LDR)

- The relationship between resistance R and illumination level is highly nonlinear.
- The simplest model of such relation is:

$$R = A * E_v^{-\alpha}$$

(E_v = illumination, lux; $0.7 < \alpha < 0.9$ for CdS)

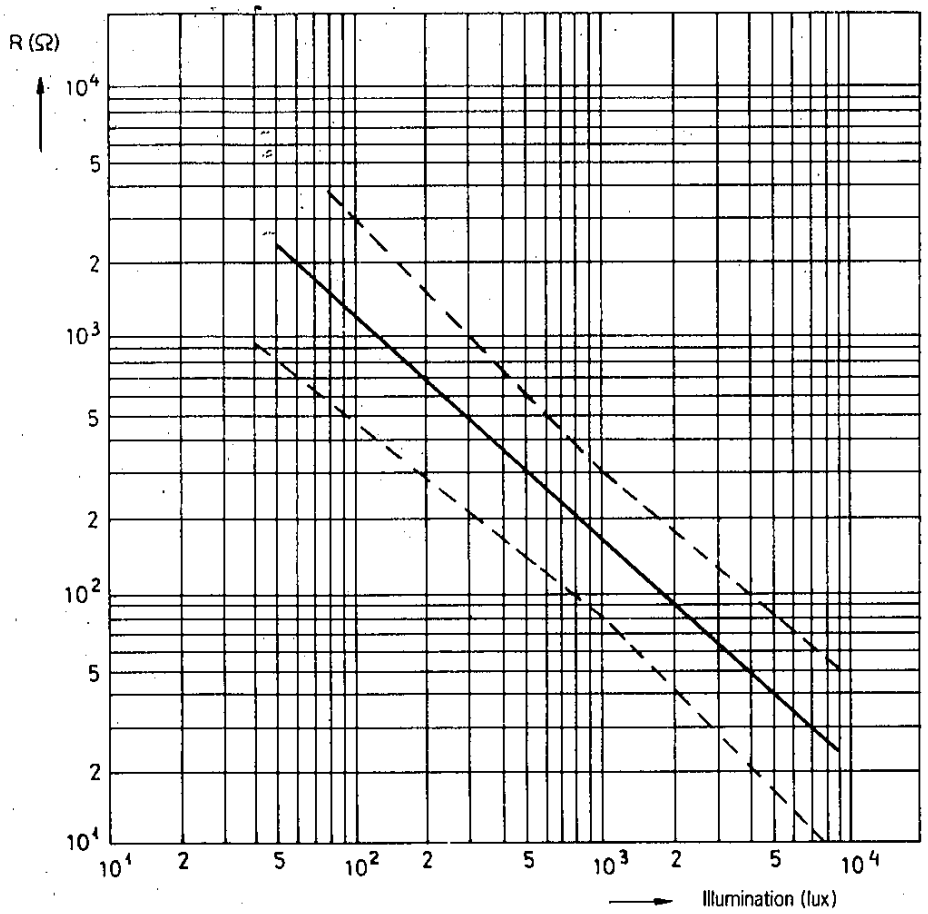

FIGURE 2.22 Resistance-illumination characteristic for a LDR (from Philips).

Light dependent resistor (LDR)

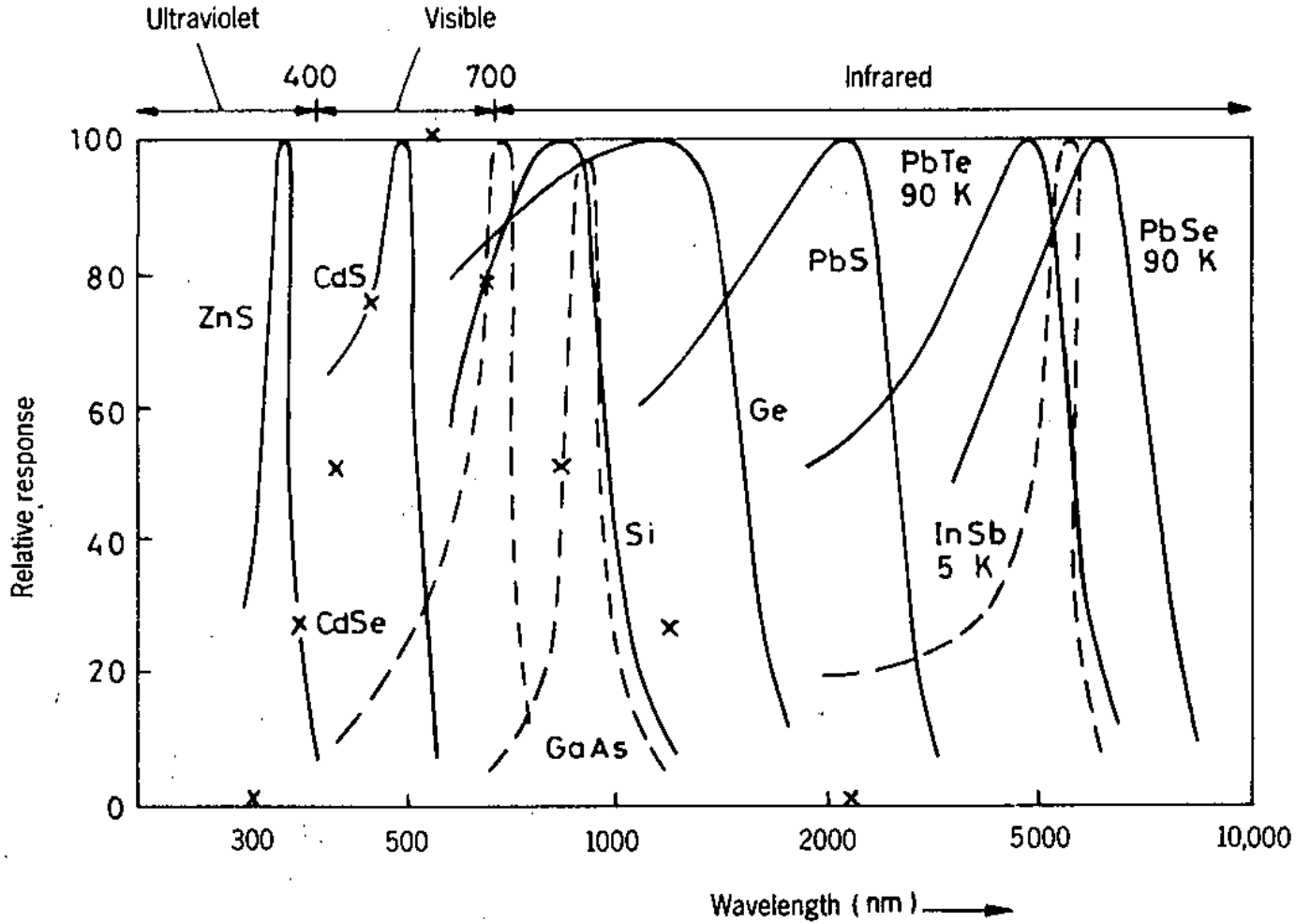

FIGURE 2.23 Spectral response for several photoconductors.

The **spectral response** of LDRs is **narrow** for various materials. Therefore the appropriate material depends on the wavelength of the radiation to be detected, taking also into account that the materials must be transparent to those wavelengths.

In the **visible range** of the spectrum (400 nm to 700 nm) and in the near infrared (700 nm to 1400 nm), cadmium-based materials are used (CdS, CdSe, CdTe). CdS has the response closest to that of the human eye.

In the **infrared** (1.4 mm to 3 mm), lead-based materials are used (PbS, PbSe, PbTe). In the medium (3 mm to 14 mm) and far (up to 1 mm) infrared, various indium-based materials (InSb, InAs), tellurium, tellurium-cadmium-mercury alloys (HgCdTe), and doped silicon and germanium are used. These long wavelengths are out of the range for photodiodes

TABLE 2.7 Some Characteristics of Visible and Infrared Light-Dependent Resistors[a]

Parameter	2322 600 9500	P577-04	J15D5-M204-S01M
Sensor material	CdS	CdS	HgCdTe
Peak response λ	680 nm	570 nm	5 μm
Dark resistance	>10 MΩ	>3 MΩ	—
Light resistance	30 Ω to 300 Ω[b]	5 kΩ to 16 kΩ[c]	—[d]
Rise time	—	45 ms[e]	—
Fall time	>200 kΩ/s[f]	30 ms[g]	5 μs
Operating temperature	−20 °C to 60 °C	−30 °C to 70 °C	77 K
Dissipation	<0.2 W at 40 °C	0.3 W at 25 °C	20 mA bias current

[a] The 2322 600 9500 is from Philips, the P577-04 is from Hamamatsu, and the J15D5-M204-S01M is from Perkin Elmer Optoelectronics.

[b] At 1000 lx.

[c] At 10 lx.

[d] Typical sensitivity is 2×10^3 V/W.

[e] From darkness to 10 lx.

[f] From 1000 lx to darkness.

[g] From 10 lx to darkness.

Light dependent resistor (LDR)

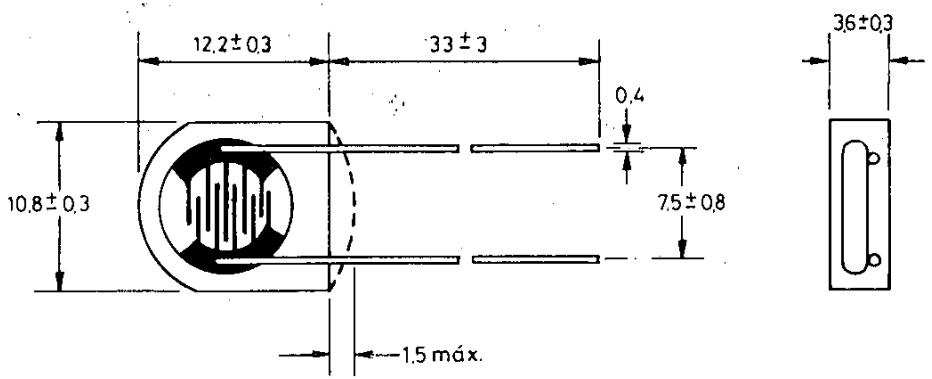

FIGURE 2.24 Low-cost LDR encapsulated in transparent plastic. All dimensions are in millimeters (Philips)

LDRs: applications
low-precision low-cost light measurement

Automatic brightness and contrast control in TV receivers, diaphragm control in photographic cameras (exposure meters), dimmers for displays, automatic headlight dimmers in cars, flame detection, and street lamp switching.

LDRs: applications that use light as a radiation to be modified

Control applications need LDRs with a steep slope in their resistance-versus-illumination characteristic. Measurement applications need LDRs with shallow slopes and include:

presence and position detection, smoke detection, card readers, burglar alarms, object counters for conveyors, optocouplers, density of toner in photocopying machines, densitometers (determining optical or photographic density), colorimetric test equipment, and tank level measurements that rely on a transparent tube. High performance photoconductors such as HgCdTe are used for thermal imaging, night vision, missile guidance (by tracking hot exhaust gases), CO_2 laser detection, and infrared spectroscopy

Magnetoresistors

A magnetic field **H** applied to a current-carrying conductor exerts a Lorentz force on electrons:

$F = -q \mathbf{v} \times \mathbf{H}$

where q is the electron's charge and v is its velocity. This force deviates some electrons from their path.

If the relaxation time due to lattice collisions is relatively short, electron drift to one side of the conductor yields a transverse electric field (Hall voltage) that opposes further electron drift.
→ Hall effect → Hall sensors

If that relaxation time is relatively large, there is a noticeable increase in electric resistance, termed the **magnetoresistive effect**. Lord Kelvin first observed this effect in iron and nickel in 1856.

Anisotropic magneto-resistive (AMR) effect

In most conductors the magnetoresistive effect is of a second order when compared to the Hall effect. But the resistance of anisotropic materials, such as ferromagnetics, depends on their magnetic moment according to the following relationship:

$$R = R_{min} + (R_{max} - R_{min}) \cos^2 \theta$$

→ The resistance R in the direction of the current is maximal for a magnetization parallel to the current and minimal for a magnetization transverse to the current.

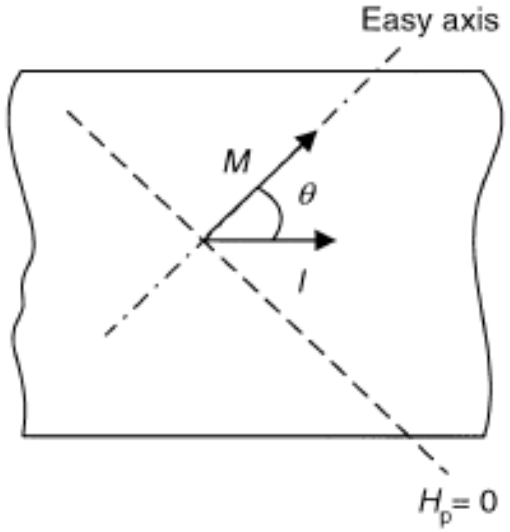

The resistance of an anisotropic material depends on the direction of its magnetization, set during manufacturing along the so-called easy axis.

Anisotropic magneto-resistive (AMR) effect

An external magnetic field causes the magnetization vector to rotate and changes angle θ, hence the resistance, depending on the field strength. The relation between change in resistance and magnetic field strength is not linear.

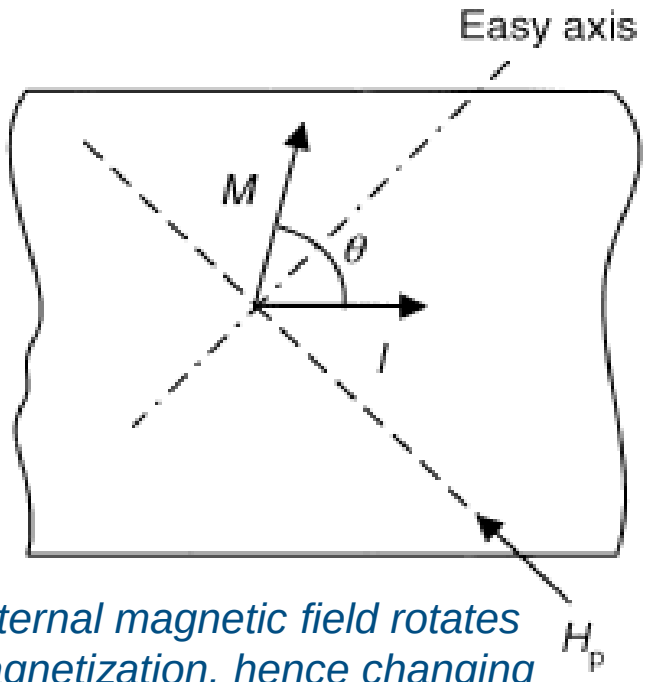

An external magnetic field rotates the magnetization, hence changing the resistance

For a field normal to the current, that relation is quadratic:

$$R = R_{min} + (R_{max} - R_{min})\left[1 - \left(\frac{H}{H_S}\right)^2\right]$$

where H_S (≥H) is the external field strength needed for a 90° rotation of the magnetization from the direction of current (saturation field).

Anisotropic magneto-resistive (AMR) effect

A bias field achieving a 45° rotation between the magnetization and the current direction yields a response

$$R = R_{min} + \frac{(R_{max} - R_{min})}{2} + (R_{max} - R_{min})\frac{H}{H_S}\sqrt{1 - \left(\frac{H}{H_S}\right)^2}$$

Which is approximately linear for $H/H_S \ll 1$.

The quotient $\frac{(R_{max} - R_{min})}{R_{min}}$ is termed the *magnetoresistive ratio.*

Note: The magnetoresistive effect is also a first-order effect in semiconductors because of the maxwellian distribution of electron velocities. Only electrons traveling at the average velocity have their Lorentz force balanced by the Hall field.

Other electrons drift transversally, thus reducing the longitudinal current, hence increasing resistance. In weak magnetic fields, the change in resistance is proportional to the square of the magnetic field component perpendicular to the direction of the current

Giant magneto-resistive (GMR) effect

The GMR effect was first observed in 1988 in multilayered structures made up from alternating layers of magnetic and nonmagnetic materials.

In magnetic materials, conduction electrons with spin parallel to the magnetic moment of the material scatter much less than those whose spins are antiparallel to the magnetic moment.

The 2007 Nobel Prize in Physics was awarded to Albert Fert and Peter Grünberg for the discovery of GMR.

Giant magneto-resistive (GMR) effect

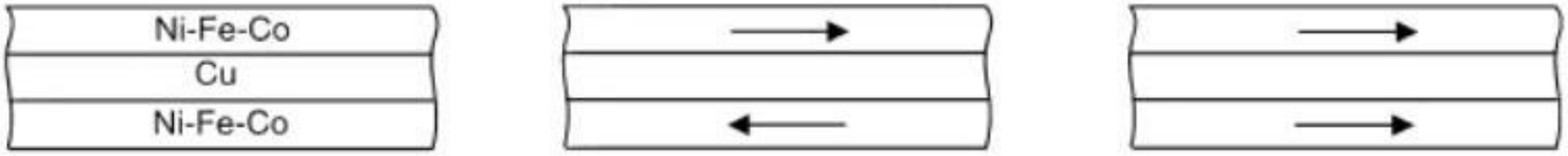

(a) (b) (c)

(a) Two ferromagnetic layers are separated by a nonmagnetic conductor. The thickness of the layers is much less than the free path of conduction electrons in the bulk material. Therefore, the conductivity is determined by scattering at the boundaries rather than bulk scattering.

(b) If in the absence of an external field the two magnetic layers have opposite magnetic moments, electrons randomly moving from one layer to the other are scattered at one of the boundaries, because their spin is aligned with the field of either one or the other layer. The structure has high resistance.

(c) If an external field is strong enough to align the fields of the magnetic layers, and the atomic lattice of the nonmagnetic interlayer matches that of the magnetic layers, the resistance decreases because electrons with spin parallel to the field can freely move in both magnetic layers. The change in resistance is up to 70% in some experimental devices.

If we ignore the need for linearization and the thermal dependence of the resistance, anisotropic magnetoresistors (AMRs) and giant magnetoresistors (GMRs) offer several advantages compared to other magnetic sensors. First, their mathematical model is a zero-order system. This differs from inductive sensors, whose response depends on the time derivative of magnetic flux density.

When compared with Hall effect sensors, which also have a zero-order model and measure without contact, magnetoresistors show increased sensitivity, temperature range (-55°C to 200 °C), and frequency passband (from dc to 5 MHz and even 100 MHz, compared with 25 kHz for common Hall effect sensors).

Unlike Hall sensors, magnetoresistors are insensitive to mechanical stress, so they can be injection-molded to form subassemblies including electronics and magnet, if needed. Their greater sensitivity means that they can operate with larger air gaps than Hall sensors. On the other hand, they saturate at lower field strengths and are more expensive.

Inertial sensors

- accelerometer measures **linear acceleration** (m/s^2)
- magnetometer measures **magnetic field strength** in uT (micro Tesla) or Gauss (1 Gauss = 100 uT)
- gyroscope measures **angular velocity** in degrees/sec

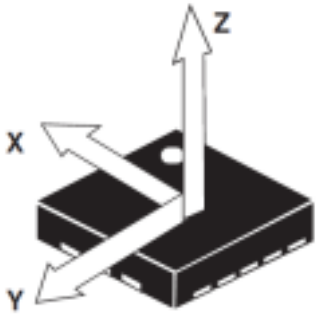

Accelerometer

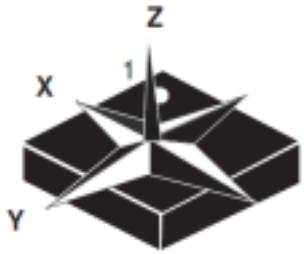

Magnetometer

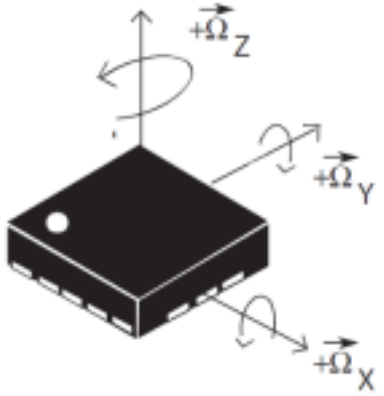

Gyroscope

Piezoresistive accelerometers / gyroscopes

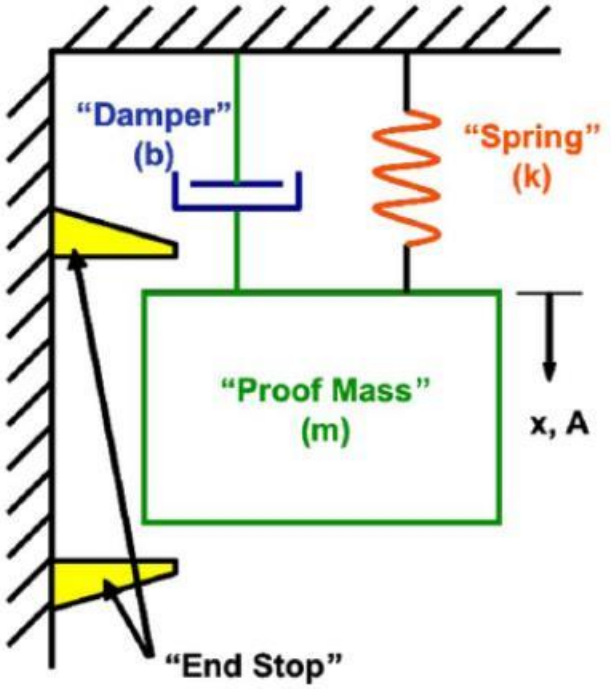

Fig. 25. *An accelerometer is modeled as a second order system with a proof mass (m), spring (k), and damper (b). The displacement (x) is proportional to the acceleration (A) in the x-direction. The range of the proof mass movement is limited by the end stops, which protect the device from shock damage.*

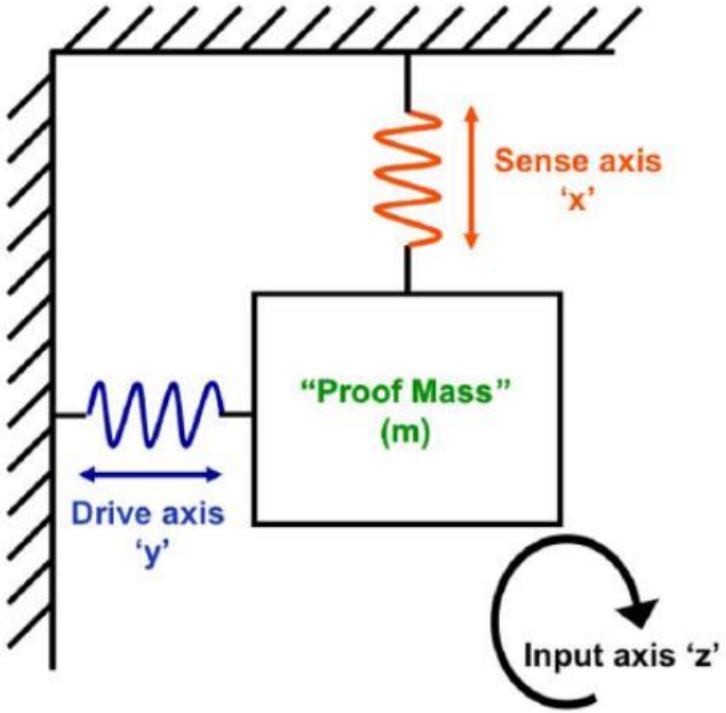

Fig. 27. *A MEMS gyroscope is driven in one axis and sensed in an orthogonal axis.*

Gyroscopes

Inertial gyroscopes measure rate of rotation and operate by detecting inertial resistance to changes in velocity, e.g., by detecting precession forces when tilting a spinning mass or via Coriolis forces on a vibrating mass.

Most micromachined gyroscopes are based on vibration and use the transfer of energy between two orthogonal vibration modes via the Coriolis force. The Coriolis force, F_c, induces acceleration (in y) of the mass proportional to vibration velocity (in x) and angular rate of rotation (about z):

$F_c = -2\, m\, \Omega\, X_{ip}\, \omega_r \cos(\omega_r t)$,

where m is mass of the proof mass,

Ω is magnitude of a rotation vector,

$X_{ip}\, \omega_r \cos(\omega_r t)$ is the in-plane velocity of the proof mass.

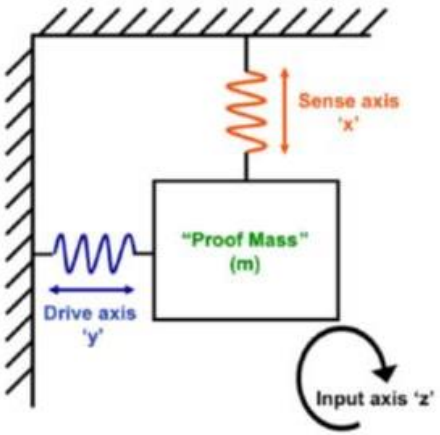

Gyroscopes

Micromachined gyroscopes are difficult to manufacture because they require a high performance resonator and an accelerometer coupled in a high-vacuum hermetic package. Few MEMS gyroscopes utilize piezoresistive detection but these require another transduction method for the vibration

For example, piezoresistive sensing can be obtained in a tuning-fork gyroscope driven by piezoelectric and electromagnetic forces.

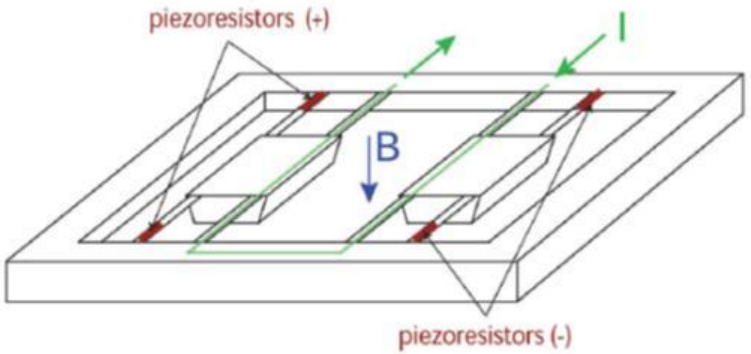

(a)

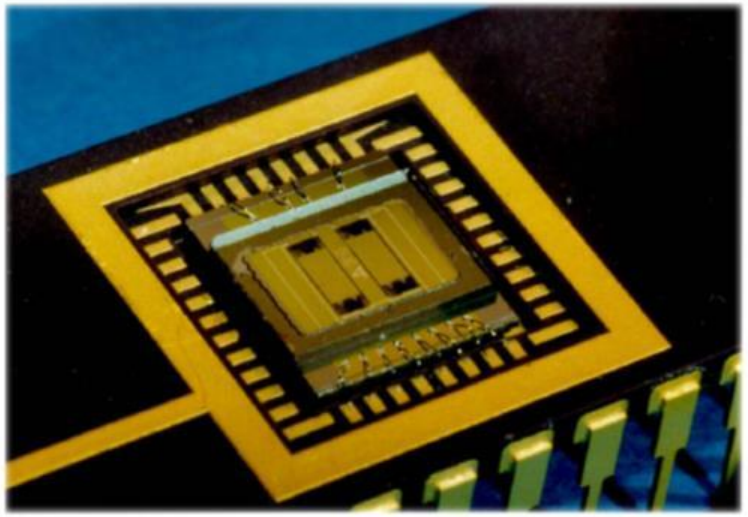

(b)

Fig. 28. *Gyroscope with electromagnetic excitation and piezoresistive detection. From Paoletti [278].* © *1996 IEEE.*

Magnetometers

Based on magnetoresistors or Hall effect sensors

Measure earth's magnetic field in Gauss or uT
- 3 orthogonal axes = vector pointing along the magnetic field
- actual direction depends on latitude and longitude
- distortions due to metal / electronics objects in the room or in HMD

advantages:
- complementary to accelerometer

problems:
- affected by metal, distortions of magnetic field
- need to know location, even when calibrated (e.g. GPS)

together with gyro + accelerometer = 9 DOF sensor fusion

MPU-9250 Nine-Axis (Gyro + Accelerometer + Compass) MEMS MotionTracking™ Device

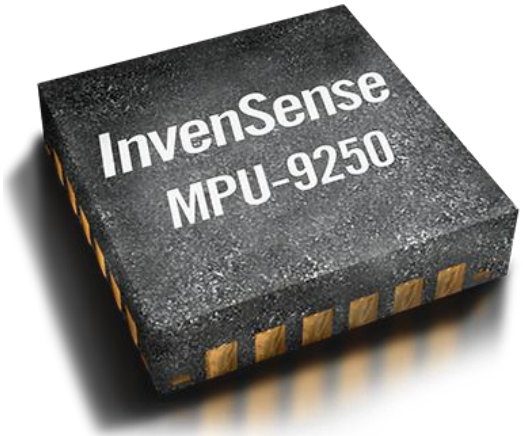

9-axis MotionTracking device for smartphones, tablets, wearable sensors, and other consumer markets.

3x3x1mm package(world's smallest 9-axis MotionTracking device)

It is a System in Package (SiP) that combines two chips: the MPU-6500, which contains a 3-axis gyroscope, a 3-axis accelerometer, and an onboard Digital Motion Processor™ (DMP™) capable of processing complex MotionFusion algorithms; and the AK8963, the market leading 3-axis digital compass.

- accelerometer low power mode (6.4μA)
- compass data resolution of 16-bits (0.15 μT per LSB). The full scale measurement range of ±4800μT helps alleviate compass placement challenges on complex pcb's
- software drivers are fully compliant with Google's Android 4.1
- MotionFusion and run-time calibration firmware

to host:
serial via USB

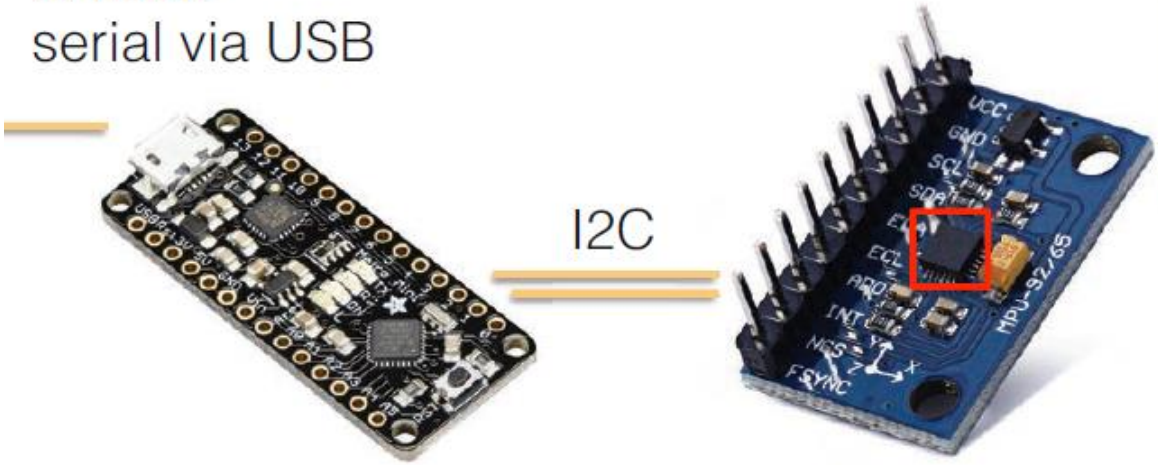

Arduino

InvenSense MPU-9255